DEVELOPMENT OF AN ADAPTIVE WEIGHT UNIT

by

ROBERT J. TARRY

Submitted to the Department of Electrical Engineering in partial fulfilment of the requirements for the degree of Master of Science.

Department of Electrical Engineering
Faculty of Pure and Applied Science,
The University of Ottawa,
Ottawa, Canada.

1964

Approved for the Department
of Electrical Engineering

Supervisor

Chairman of the examining committee

Chairman of the Department

ABSTRACT

The subject of this thesis is the design and evaluation of an adaptive weight unit based on the transfluxor magnetic core.

The search for multi-level or analog storage devices has led to the study and development of many different types of storage mechanisms, ranging from mechanical and chemical devices to magnetic core devices. This thesis presents the characteristics of a special type of magnetic core, called the transfluxor, used as an adaptive weight element.

Design criteria and limits have been established and the relationship of component tolerance and stability of operation is discussed.

A number of weight units were constructed and were used in conjuction with a threshold logic unit in order to demonstrate the dynamic characteristics of the weight units. Simple tests were carried out on this system and the results are presented.

Conclusions are drawn as to the success of the design.

ACKNOWEDGEMENTS

The author wishes to thank Professor G.S. Glinski, Chairman of the Department of Electrical Engineering, who supervised this research project.

My thanks for financial assistance are due to the Defence Research Board (Grant No. 9931-10) and to the National Research Council (Grant No. A-875).

PREFACE

The initial work performed on this thesis was in the direction of completing the project undertaken by P. Deschenes(1).

However, this author soon formed the opinion that a better solution to the adaptive weight problem could be found in the use of the transfluxor. Consequently, the herein reported system was designed and tested.

CONTENTS

CHAPTER I

INTRODUCTION

1. General Comments

The author assumes that the reader is familiar with the field of learning or adaptive machines, at least to the extent of understanding the basic principles of threshold logic (2) (3) (4) and of the Perceptron machine (5) (6) (7) and Adaline machine (8) (9).

The primary purpose of the project reported in this thesis was to develop an adaptive weight unit whose value could be quickly and automatically adjusted. In order to set the required characteristics of such a unit it was found necessary to have data concerning the system in which the weight unit would be employed. Such a system did not exist and so it was found necessary to select a system which would provide a measure of the performance of the adaptive weight and would demonstrate the principles of automatic adaptation. In addition, it was decided that the system should be as simple as possible since the main goal was the development of the weight unit and not an adaptive system. It was decided that the system would consist of one threshold logic unit (TLU) having up to nine inputs, each input associated with an adaptive weight, and having an adaptive threshold. Such a system is relatively simple except, perhaps, for the duplication of the ten adaptive weights (one for each input plus one for the adaptive threshold) and for the duplication of necessary hardware (connectors, wiring, control circuitry, etc). The intention was to use the nine inputs in the form of a three-by-three matrix. The equipment could then be used to demonstrate adaptive procedures in the form of pattern recognition experiments. It appears now that the choice of nine inputs has been too ambitious and optimistic in the light of the results obtained on the performance of the adaptive weight. This problem will be fully discussed later in this thesis.

Regardless of the degree of success obtained for nine inputs, the equipment with slight modification, can be used for experiments in single and multi-level TLU realizations of given Boolean expressions. The latter would require one or more duplicates of the present system. The automatically adaptive weights make such experiments interesting. Another possible use for the equipment is in conjunction with an on-off control system in which case the TLU would be functioning as an adaptive digital controller (10). Finally, the design of the adaptive weight is such that each weight unit could be used alone as a multi-level memory element; that is, the units are not restricted to use only with the TLU circuitry.

The model of the TLU to be used in this thesis is shown in Figure 1. As can be seen, the threshold is treated as an additional weight, w_{n+1}, with argument $x_{n+1} = 1$ at all times. (Numerical 0 and 1 will be used to denote the logical F and T respectively). Thus, the equation governing the operation of the TLU is

$$Z = 1 \text{ iff } \sum_{i=1}^{n+1} (x_i w_i) > 0 \qquad (1.1)$$

$$= 0 \text{ otherwise}$$

2. Adaptive TLU

The system developed in the course of this project is basically the same as the device in Figure 1, except that each weight is an adaptive weight of the form shown in Figure 2. When adaptive weights are used, the TLU will be referred to as an adaptive threshold logic unit, abbreviated as ATLU.

In general, there are two major phases or modes of operation for adaptive machines. The first is the training or adapting phase during which the machine is presented with a selected subset of the input set. The two most popular and obvious ways of training the machine on this

subset are to either force the machine to respond correctly to a member of the subset before another member is presented or, to present each member in order, causing small changes in the machine parameters which, after a number of repetitions of the subset, will cause the machine to converge to a solution, if one exists. There are, of course, endless variations of these two schemes. The former method is the one which has been chosen for use in this equipment.

The second phase of operation is either a test phase during which the ATLU is "examined" to see how well trained it is or, the second phase can be an operate phase in which the ATLU is used to perform some logical operation, either alone or in some digital system. The ADAPT LOGIC block in Figure 2 is active only during the training phase.

There are many possible adaptation schemes which could be used to decide when, in what direction, and by what amount the weight is to be changed (11) (12) (13). The majority of these are very complicated and would be extremely difficult, if not impossible, to automate. The method used in this machine is that if the ATLU correctly maps the input, then the weights remain unaltered. If the output of the ATLU is incorrect, the weight associated with each active input is repeatedly incremented in such a direction so as to produce a correct response. At the same time, the inactive input weights are incremented in the opposite direction. The scheme is best expressed by the following equation

$$w_i(t+1) = w_i(t) + \Delta w \left[f_{I_i}(t) - f_{D_i}(t) \right] \qquad (1.2)$$

$$i = 1, 2, \ldots, n$$

$w_i(t)$ - value of the i^{th} weight at time t.

Δw - a small, fixed increment in w.

$f_{I_i} = f(P, Z, D, x_i)$

$f_{D_i} = f(P, Z, D, x_i)$

If $f_{I_i}(t) = 1$ then w_i is incremented by the amount Δw in the interval between t and (t + 1). Similarly, if $f_{D_i}(t) = 1$ then w_i is decremented by the amount Δw in the interval between t and (t + 1). The functions f_{I_i} and f_{D_i} are disjoint. Their functional relationships are given in Figure 3. Thus,

$$f_{I_i} = [(\bar{z} D x_i) \vee (z \bar{D} \bar{x}_i)] P \tag{1.3}$$

$$f_{D_i} = [\bar{z} D \bar{x}_i) \vee (z \bar{D} x_i)] P \tag{1.4}$$

3. Adaptive Weight Characteristics

The advantage of adaptive weights is obvious but, unfortunately, their physical realization is not. An adaptive weight should possess as many as possible of the following characteristics:

1. wide, linear range
2. long-term storage
3. non-distructive readout
4. ease of incrementation
5. temperature, aging and other enviromental stabilities
6. small physical size
7. simplicity of design
8. low cost

The question of operating speed can only be answered by considering the operating speed of the system in which the weight unit is to be used. For example, in a visual pattern recognition system an inexpensive, slow responding weight such as a mechanical or chemical device would suffice. On the other hand, a high speed system would require a faster, more costly weight, using, for example, a magnetic core as the memory element.

Many devices have been investigated (14) which possess some of the above characteristics but, there has not been a simple, inexpensive solution to the problem. The comparison of different types of weights is often misleading because the investigator has failed to mention the complexity and cost of the circuitry associated with a particular type of weight element. In some cases the cost of this circuitry is many times that of the weight element and is often the governing economic factor.

The ideal operating characteristic of the adaptive weight is shown in Figure 4 where

y = (summation of all previous increments)
- (summation of all previous decrements).

The instantaneous value of the weight, w_i, is a function of how often and in what direction w_i has been altered in the past. In other words, the present value of the weight is a function of its memory.

Any device which is used to realize such a characteristic curve will possibly contain in its characteristic curve, saturation regions, areas of non-linearity and/or a hysteresis effect. Also, most devices will be quasi-continuous, some exhibiting a larger number of smaller steps than others. The combination of all these defects is demonstrated in Figure 5. The characteristic curve of the weight unit developed by the author is similar to that of Figure 5 except that there is no hysteresis effect.

4. Transfluxor Principles

The element chosen as the adaptive weight in this thesis is the transfluxor, a device reported, for example, by Rajchman and Lo (15)(16). The most important property of this device is its ability to store and to provide non-destructive readout of from one to about 100 discreet values. In addition, the stored value can be changed relatively quickly and easily.

The transfluxor is a two aperture, square-loop, magnetic core and is shown in Figure 6. The material around aperture 1 is used for storage while that around aperture 2 is used as the core of a transformer whose input and output windings are windings 2 and 3 respectively. By controlling the amount of reversed flux around aperture 1, one controls the amount of flux available for switching in the "transformer" section of the core. This, in turn, affects the amplitude of the output of winding 3. The amplitude of this voltage is, after necessary processing, the desired variable, w_i.

Consider now that a large current, I_1, has been momentarily passed through winding 1 and had such a magnitude and direction that the core is completely saturated in one direction as shown in Figure 7(a) . This condition is possible since the design of the core is such that the width of leg 1 is equal to or greater than the sum of the widths of legs 2 and 3. Let there be an alternating current, I_2, flowing through winding 2. When the resultant MMF is in the counter-clockwise (ccw) direction around aperture 2, there can be no change in flux linking winding 3 because leg 2 is already saturated in that direction. Hence, there is no voltage induced in winding 3 and, the output is zero. A similar argument, involving leg 3, holds for the case when the MMF is in the clockwise (cw) direction. Under this condition the transfluxor is said to be blocked.

If now a small amount of flux is caused to be reversed around aperture 1 (Figure 7 (b)) then, when the MMF of winding 2 is in the ccw direction, this small flux can be reversed, causing a similar amount to be reversed in leg 3. Leg 2 will become saturated as in the previous case but the stored value has not been destroyed, simply transferred into leg 3. During the next half cycle of current I_2, the MMF will cause the transfer of the small flux back into leg 2 completing one cycle of operation. This process of flux transfer generates a voltage in winding 3 and thus, the device

provides permanent storage and non-distructive readout of the stored value. This transfer of flux has given rise to the name "transfluxor". The stored value can be changed by altering the flux reversed around aperture 1 and the stored value will have its maximum value when all the flux in leg 2 has been reversed due to the action of winding 1. This situation is shown in Figure 7(c) after the flux has been re-distributed due to the action of the MMF of winding 2. For a more detailed, and perhaps clearer, explanation and further characteristics, the reader is referred to references (16) and (24).

The incrementing of the flux around aperture 1 can be achieved by using the process of flux integration (17) (18). Consider a simple toroid with a square-loop hysteresis curve (Figure 8a). Faraday's law gives

$$E = - \frac{d\psi}{dt}$$

where ψ = flux linkages

and a = number of turns

Φ = flux

A safe approximation with such a core is that the flux links all of the a turns. Thus,

$$E = -a \frac{d\Phi}{dt}.$$

Neglecting the negative sign we may approximate this as

$$E = a \frac{\Delta\Phi}{\tau} \quad \text{where } \tau = \Delta t$$

or
$$\Delta\Phi = \frac{E\tau}{a} \tag{1.5}$$

If the core is initially in the state denoted as point 'a' in Figure 8(b) then, the application of a pulse of magnitude E and duration τ will result in the movement of the state to point 'b' along the indicated path.

A small amount of flux ($b - a = \Delta\Phi$) has thus been set into the core. Controlling either a, τ or E will allow the establishment of as many steps as desired between the limits of $-\Phi_s$ and $+\Phi_s$. When dealing with actual cores the process just described is altered by the fact that the core material will never have a perfectly square hysteresis loop. That is, Φ_r is less than Φ_s. The result is a smaller linear range of operation and less flexibility in the trading-off of pulse amplitude for pulse width. These imperfections were demonstrated by the core used in this equipment and the resultant effects will be discussed in more detail in later chapters.

5. Basic Limitations

Equation (1.1) represents an ideal condition and, as such, must be modified to take into account the unavoidable variations in x_i, w_i and θ that will occur in physical realizations of the circuit of Figure 1. In this machine, variations in x_i are not important because the circuitry involved with these variables is of the switching type and has been designed to compensate for large variations in x_i. The two sources of error are then the variations in w_i and the discriminator level, θ.

The level θ is fixed in the design of the equipment and is equivalent to 0 as in equation (1.1). The limits of variation of the level about this point are best described as θ_1 and θ_2; that is, the actual discriminator level will always fall somewhere in the range of θ_1 to θ_2. Variations in w_i can be considered as a percentage of the value of w_i. If 'e' is the maximum possible percentage variation in w_i, expressed as a decimal fraction, then the actual value of the weight must be written

$$w_i \pm ew_i = (1 \pm e)\, w_i$$

Applying these two refinements to equation (1.1) results in

$$Z = 1 \text{ iff } \sum_{i=1}^{n+1} (x_i w_i) - e \sum_{i=1}^{n+1} (x_i |w_i|) \geqslant \theta_2 \tag{1.6}$$

$$Z = 0 \text{ iff } \sum_{i=1}^{n+1} (x_i w_i) + e \sum_{i=1}^{n+1} (x_i |w_i|) \leqslant \theta_1 \tag{1.7}$$

Z is otherwise undefined.

The size of Δw, the fixed increment in the weight, is limited in two respects. Firstly, the number of increments required over the range of operation of a given weight is a function of the number of inputs to the ATLU. For example, Winder (19) gives the following weight vector for the minimal - integral realization of a complex function of six variables:

$$\bar{w} = (w_1, w_2, w_3, w_4, w_5, w_6, w_7)$$

$$= (18, 7, 6, 4, 3, 2, -18)$$

Thus, if W represents the maximum positive or negative value that w_i may have then, it is obvious that

$$\Delta w \leqslant \frac{W}{18}$$

in order that the function be realizable with a set of seven weights all having the same characteristics. In general, let the relationship between the number of input variables, n, and N, the maximum required number of steps over the positive or negative range of operation of the weight, be

$$N = G(n)$$

This is based on the minimal integral solution of which N is the largest positive or negative member. Unfortunately, G(n) is unknown in the general case. A number of investigators have attempted to

establish limits on G(n) but, the results have been poor, especially for smaller values of n (20). Winder (19) has provided exact answers for up to six variables. For larger values of n the best method of accounting for this unknown factor is to design for as large an N as is consistent with other restrictions. On the basis of a review of Winder's tables it appears that only the few, most complicated functions of n variables involve the maximum required value, N. Thus, on an average, a smaller number of increments is probably acceptable. In general, however, one of the restrictions on the increment Δw, is

$$\Delta w \leqslant \frac{W}{G(n)} \cdot \tag{1.8}$$

The second restriction is due to the requirement that Δw not be less than a certain minimum value in order to have stable operation. The problem is that the machine may adapt and provide the correct response at the present time but, due to variations in θ or w_i, the machine might respond incorrectly during a later test or operate phase of operation. The designer must establish the minimum size of Δw so that subsequent variation in θ or w_i does not cause a previously correct response to be altered.

An important factor in establishing this limit on Δw is the nature of the adaptive process used in the machine. In the present case, as mentioned previously, if the ATLU incorrectly responds to a certain input and the machine is in the adapt phase, then each weight associated with an active input is incremented, by Δw, in such a direction as to eventually cause a correct response. If there are m of the possible n inputs involved in the given input vector, i.e. if there are m of the n inputs with a value 1 then, the total change in the weighted sum, for every cycle of adaptation, is equal to

$$(m + 1)\ \Delta w.$$

The additional 1 accounts for the threshold. One can now set up a critical-case situation which can be used to relate the size of Δw to the nature of the adaptive process and to the variations in θ or w_i.

Let there be a particular input n-tuple, S_1, with its associated weighted sum, Σ_1. Let this input involve m of the n possible variables and be such that the weighted sum, with all possible errors considered, is just equal to θ_1. This is the largest weighted sum which will, without error, give Z = 0. The equation for this case is

$$\sum_{j=1}^{m+1} (x_j w_j) + e \sum_{j=1}^{m+1} (x_j |w_j|) = \theta_1$$

where the index j has been assigned to only the m active input variables and their associated weights. The situation is illustrated in Figure 9(a).

Suppose now that the machine, in the state shown in Figure 9(a), is presented with the same input, S_1 which the operator of the machine wishes to now be classified as Z = 1. The machine will respond incorrectly and the adaptive process must change the weighted sum, Σ_1, to a new value, Σ_2, so that

$$\sum_{j=1}^{m+1} (x_j w_j) - e \sum_{j=1}^{m+1} (x_j |w_j|) = \theta_2$$

This situation is shown in Figure 9(b).

For stable operation Σ_1 must be changed to Σ_2 under the action of only one cycle of adaptation. Suppose, instead, that Σ_2 is some point in between θ_1 and θ_2. It is possible that the discriminator level is at the value θ_1 and thus, the machine would respond correctly indicating successful adaptation. If the level later moves to θ_2 then an incorrect response would result. In changing from Σ_1 to Σ_2 the number of increments in the weighted sum is

$$(m + 1)\ \Delta w$$

This amount must be greater than or equal to the difference between Σ_1 and Σ_2. That is,

$$(m+1)\,\Delta w \geq (\theta_2+\theta_1) + e\left[\sum_{j=1}^{m+1}(x_j|w_j|) + \sum_{j=1}^{m+1}(x_j|w_j|)\right] \qquad (1.9)$$

Inequalities of this type have been used to draw conclusions as to the maximum permissable value of the sum of the absolute value of all the weights. However, in this case we are attempting to set a limit on Δw and to do so we must supply a value for the various $\Sigma x_j|w_j|$ terms in equation (1.9). The most extreme case is when each weight is at its maximum value W and $\frac{m+1}{2}$ of the weights are negative and the remainder are positive, resulting in a weighted sum close to zero. Equation (1.9) then becomes

$$(m+1)\,\Delta w \geq (\theta_2+\theta_1) + e|W|[(m+1)+(m+1)]$$

and,

$$\Delta w \geq \frac{(\theta_2+\theta_1)}{m+1} + 2\,e\,W \qquad (1.10)$$

Thus, the lower limit on Δw is found when $m = 1$, the lowest value m assumes. Therefore,

$$\Delta w \geq \frac{(\theta_2+\theta_1)}{2} + 2\,e|W| \qquad (1.11)$$

In the vast majority of cases the values of the individual w_i are less than the maximum value of W and a correspondingly smaller Δw could be tolerated. However, to ensure correct operation under all possible conditions, equation (1.11) should be used.

Suppose now that there is an input whose weighted sum is considerably less than θ_1 and that the operator wishes to change the response to that particular input from Z=0 to Z=1. At first, this

situation would appear to be more strict than the one which resulted in equation (1.11) since the corresponding equation for Δw would be

$$\Delta w \geqslant \frac{(\theta_2+\theta_1)}{m+1} + 2\,e\,|W| + \frac{k}{m+1}$$

where k is the amount that the weighted sum, Σ_1, is below the level θ_1. If this analysis is carried to its logical conclusion we would have to consider the case where all m weights where at their maximum negative values i.e. $k = m\,|W|$.
This would result in

$$\Delta w \geqslant \frac{(\theta_2+\theta_1)}{m+1} + 2\,e|W| + \frac{m}{m+1}\,|W|$$

The predominant term is

$\frac{m}{m+1}\,|W|$ and it has a maximum value of $|W|$ for large m.

Such a condition would leave us with only two steps over the entire range of operation of the weight. The answer to this dilemma is that the movement of the weighted sum from $-m|W|$ to θ_2 does not take place in one cycle of adaptation but instead, requires many cycles. For each cycle the weighted sum increases a small amount, $\Delta w\,(m+1)$, until it reaches the position shown in Figure 9(a). That is, one assumes that whatever the initial value of the weighted sum a small, regular increase is made each cycle of adaptation until the sum reaches the value shown in Figure 9(a). Such an assumption is consistent with the small Δw required by equation (1.8).

To conclude, the limits on the size of Δw, from equations (1.8) and (1.11) are

$$\frac{|W|}{G(n)} \geqslant \Delta w \geqslant \frac{(\theta_2+\theta_1)}{2} + 2e\,|W| \qquad (1.12)$$

This analysis has been included in this introductory chapter to illustrate the dependence of weight parameters, such as $|W|$, Δw and e, upon

system parameters, such as n and $(\theta_2+\theta_1)$. In Chapter III, equation (1.12) will be used, along with measurements of some parameters, to evaluate the capabilities of the weight unit and system designs which are discussed in the following section, Chapter II.

CHAPTER II

CIRCUIT DESIGN

1. Discussion of Block Diagrams

The block diagrams of the system and the weight unit are shown in Figure 10 and in Figure 11 respectively. A signal time chart is provided in Figure 12. This chart includes the time relationships of the more important signals in the above two block diagrams, for three typical cycles of operation.

In the block diagram of the system, all blocks are common to every weight unit. The input variables, x_i, the output, Z, and the clock signal are synchronous, pulse-type signals with a frequency of 2.5 kc/s and a pulse width of 200 μs. The AC input signal has a frequency of 5 kc/s and is synchronized with the system clock. The Threshold Gate provides a variable-width pulse output signal and the Output Pulse Generator is used to convert this signal into a pulse having the standard, 200 μs width. The two signal amplifiers condition the D (desired output) and Z (actual output) signals for application to all of the weight units. The Increment Pulse Generator supplies the adapt pulse, P, at the clock frequency and the Training Controls control the phase or mode of operation of the equipment. The three modes of operation are entitled Adapt, Operate and Erase. In the application of the machine as a simple pattern recognizer, the input variables, x_i, and the clock are both derived from the same external pulse generator. Each x_i is controlled by an individual switch, located on the Display Panel. The AC signal is obtained from an external generator and the synchronization of the AC signal and the clock signal takes place external to the machine. The Display Panel indicates the state of each x_i variable and the state of the D and Z variables.

The weight unit block diagram shows the circuits directly associated with the transfluxor core. The Input Signal Buffer provides isolation for the input variable and also provides the x_i and $\bar{x}_i$ variables, as shown. The Adapt Logic Circuit is thus provided with all the variables involved in equations (1.3) and (1.4). The Adapt Logic Circuit applies a pulse, of the proper amplitude, polarity and duration, to winding 1 when the machine is in the process of adapting. The AC Input Circuit suitably transforms the 5 kc/s signal into the proper shape for providing the carrier signal for the transfluxor. The Holding Circuit was found to be necessary due to an undesirable, but unavoidable, property of the core. This property will be fully discussed later in this chapter. The Output Gate serves two purposes. It provides a simple gate for w_i which is synchronized to x_i; that is, the multiplication, $x_i w_i$, takes place in this gate. The second function of the gate is to add in a negative bias so that the value of $x_i w_i$ may take on negative values. The output of winding 1, and of the Holding Circuit, is always positive and, consequently, a negative bias must be supplied in order to have w_i range over negative as well as positive values.

Different methods of using the transfluxor have been suggested (21), (22) (23) and there has also been progress in the use of similar MAD (multiaperture device) cores in systems of only wire and cores (24). The latter method appears to be one of the most economical systems for realizing ATLU's.

2. Transfluxor Circuit Design

This section of Chapter II deals with the characteristics of the core used in this equipment and with the design of the circuitry associated with the core. The transfluxor operating principles presented in Chapter I were meant only as a brief introduction to the subject. The detailed operating characteristics are much more

complicated, as will presently be shown.

Physical dimensions of the core are given in Figure 13. The particular core used was chosen on the basis of low cost and availability. The core was custom produced and is three times the physical size of the core used in reference (16). This was done in order to provide large apertures which would allow a maximum of flexibility in the type and size of windings placed on the core. It was realized that the operating speed would suffer due to the relatively large physical size, but speed was not considered as one of the most important operating characteristics. The cores could be used at speeds considerably greater than the chosen 5 kc/s but more design problems would be encountered. A relatively low operating speed is desirable in that pulses of longer duration may be used and, these signals can be easily handled by inexpensive germanium transistors and diodes with relatively little distortion resulting from turn-on and turn-off time delays.

AC Input Circuit

Consider once again Figure 6 and Figure 7. The mode of operation used in this design was to supply winding 2 with a high frequency, AC signal which would cause the continual transfer of stored flux between leg 2 and leg 3, as previously explained. For proper operation, the MMF of winding 2, when in the ccw direction, must be of sufficient amplitude to cause flux reversal around aperture 2, but must not be so large as to reverse flux through leg 1. Such a reversal would destroy the level stored around aperture 1.

The portion of the AC input signal which generates this ccw MMF is referred to as the "prime" cycle, for it is during this time that the stored value of flux is transferred to leg 3 in preparation for the following "drive" cycle, which is the one which

generates the useful output in winding 3. There is no limit on the magnitude of the MMF of winding 2 during the drive cycle because, as soon as the stored flux has been returned to leg 2, leg 3 saturates and there can be no further flux change caused by the MMF of winding 2. It is advantageous to have a larger current change in winding 2 during the drive cycle than during the prime cycle, since such an arrangement provides for faster flux change during the drive cycle and consequently, the voltage induced in winding 3 has a larger peak amplitude. Figure 14 shows the effect of the magnitude of the MMF of winding 2 on the flux stored in leg 1. The core was initially put in the blocked condition and the MMF was increased until flux reversal in leg 1 occurred, as indicated by an increase in the voltage induced in winding 3. As can be seen, if the MMF exceeds 0.70 ampere-turns (AT) there will be flux reversal in leg 1. The value of 0.70 AT is much more than is necessary for proper priming of the core because, this value corresponds to a path through leg 1 and leg 3 whereas, the path through leg 2 and leg 3 is much shorter. Comparison of the length of these two paths, based on the data of Figure 13, indicates that a value of 0.40 AT is sufficient for proper priming. A value of 0.45 AT was consequently chosen.

The value of the MMF during the drive cycle was set at approximately three times the value of the prime MMF. This value corresponds to the maximum acceptable value of current and heat dissipation in the associated circuits.

The AC Input Circuit diagram is given in Figure 15. Winding 2 was set at 10 turns to conserve space in aperture 2 and simple calculations will show that when T1 and T2 are, in turn, saturated that the prime and drive MMF's are 0.45AT and 1.20AT respectively. The AC input signal is controlled by R1 which effectively controls the rise time of the current in winding 2. Transistors T1 and T2 dissipate

power only during the time that the base voltage is between +12 and -12 volts and consequently operate within the 150 mw collector dissipation rating.

Holding Circuit

The Holding Circuit diagram is shown in the left-hand portion of Figure 16. The widest operating range for E_o is obtained with a high impedance load on winding 3 and T1 and T2 provide such a load. Diode D1 and capacitor C1 form a holding network which is used to hold the peak value of E_o for a short period of time. This circuit is necessary due to a shift in the peak value of E_o for different stored levels. Figure 11, on page 327 of reference (16), illustrates this effect and, Figure 17 of this thesis shows similar results obtained for tests on the present core.

In general, the w_i will all differ in value and, if the peak values of the corresponding E_o's are to be added simultaneously, then the lower valued ones, which occur first, must be either delayed or the peak value held until all the E_o's have reached their respective peak values. A delay circuit would be far too complicated since the amount of delay required is a function of the amplitude of E_o. The simplest possible arrangement is a peak detecting circuit and this was the type chosen. It should be pointed out at this point that the weighted sum is not considered to have occurred until all the E_o's have reached their respective peak values. This occurs at the time when the E_o corresponding to the highest valued weight reaches its peak value. At that time the weighted sum is at its maximum value and may or may not exceed the triggering level of the threshold gate, as expressed by equation (1.1). As shown in Figure 17, the maximum holding time required, for a range of operation from 5 to 25 volts, is 7 μs.

In the ideal case, neglecting the reverse leakage currents of D1 and T3, the discharge time constant of the network C1, R2 and R3 would be

$$TC = (10 + 2.2)10^{3} \times 0.2 \times 10^{-6}$$

$$= 2.44 \times 10^{-3} \text{ seconds}$$

The held value will thus drop off at a relatively slow rate as shown in Figure 18. The error introduced in the value of a weight, due to this drop off, will be greatest when the weight has the lowest possible value (thus occurring earlier in time) and another weight has the largest value possible, resulting in the maximum time difference of 7 μs. The resultant error in the low value weight can be calculated as follows:

$$E_1 = E_o \exp^{-\frac{t}{RC}}$$

$$\text{error} = \frac{E_o - E_1}{E_o}$$

$$= \frac{E_o - E_o \exp^{-\frac{t}{RC}}}{E_o} \times 100\%$$

$$= (1 - \exp^{-\frac{t}{RC}}) \, 100\%$$

$$\text{error} = \frac{t}{RC} \times 100\% \quad \text{for } t \ll RC$$

Thus, the maximum theoretical error due to the discharge of the holding network is

$$\frac{7 \times 10^{-6}}{2.44 \times 10^{-3}} \times 100 \approx 0.30\%$$

The measured sag on a signal of 18.5 volts was 0.08 volts over

the initial 7μs portion. This corresponds to an error of

$$\frac{0.08}{18.5} \times 100 = 0.43\%$$

The difference between this and the theoretical value can be attributed to reverse leakage currents in D1 and T3, and to measuring errors.

This error would only become significant if it was equal to or greater than Δw. For example, the maximum error for a 5 volt signal is $5 \times 0.0043 = 21.5 \times 10^{-3}$ volts. This is also the maximum amount of error in any weight value for, as the magnitude of the weight increases the required holding time decreases in the same proportion. This circuit would operate satisfactorily in a system with $\Delta w \geqslant 21.5 \times 10^{-3}$ volts. For the present operating range of approximately 20 volts this would be equivalent to

$$\frac{20}{21.5 \times 10^{-3}} \approx 1000 \text{ steps}$$

over the entire range of the weight. The largest number of steps anticipated is less than 100 and the error is therefore negligible.

Output Gate

The remaining portion of Figure 16 is the diagram of the Output Gate circuitry. The purpose of this gate is 1) to provide a current porportional to E_1 2) to add in a negative bias current so that the weight value, now represented by a current, can take on negative as well as positive values and 3) to provide a simple gating action which results in the multiplication, $x_i \ w_i$.

One of the desired features of the machine was that the addition or removal of weight units should not affect the value of the

threshold or the value of other weights. It was decided that a grounded base amplifier would be used in view of its low input impedance and inherent stability. The amplifier used (T1 of Figure 19) has a measured input impedance in the neighbourhood of 40 ohms. For the purpose of calculations, the output ends of resistors R3 and R9 of Figure 16 can be considered at ground potential. If transistors T3 and T4 are both OFF then, neglecting the reverse leakage currents, the positive output current is

$$I^{+} = \frac{E_1}{R_2 + R_3}$$

and the negative output current is

$$I^{-} = \frac{-24}{R8 + R9}$$

The total output current is

$$I_T = I^{+} + I^{-}$$

$$\therefore \quad I_T = \frac{E_1}{R2 + R3} - \frac{24}{R8 + R9} \qquad (2.1)$$

E_1 ranges from approximately +5 volts to a maximum of +24 volts. The four resistances involved must be chosen so that a value of $E_1 \approx$ 15 volts results in $I_T \approx 0$. In addition, R3 and R9 should be made as large as possible, with respect to the input impedance of the summing amplifier, so as to reduce interaction between weight units. On the other hand, R2 and R8 must be of sufficient value as to limit the collector currents of T3 and T4 to such values that reasonable base currents will saturate these transistors. Resistor R2 limits the maximum steady-state current which flows through T2, (when T3 is ON) and this resistor must be of a high enough value so as to safely limit the collector dissipation of T2. For example, suppose

T3 is ON and E_o = 15 volts. Collector dissipation of T2 is then

$$P = E_{ce} \cdot I_c \text{ watts}$$

$$= (24 - 15) \left(\frac{15}{R2}\right)$$

The rating on the transistor is 150×10^{-3} watts so that

$$R_2 \geq \frac{150}{150} \times 10^3 \text{ ohms}$$

or, R2 should be greater than 1000 ohms. This is the most critical case and R2 was set at 2200 ohms as an added precaution. The other values chosen are as shown in the diagram.

T3 and T4 function as shunt-type gates. When both transistors are saturated the output current is zero, neglecting the collector - emitter saturation voltage of T3 and T4. A timing problem exists in this circuit in that T3 and T4 should operate simultaneously. This never happens, of course, and consequently, C2 was added to insure that T4 operates before T3. By doing so, the actual value of w_i will always be approached from the negative side as the output gate is turned ON. Finally, T3 serves the purpose of discharging capacitor C1 every cycle of operation. If E_1 was not reduced to a low value before a cycle of operation, it is possible that E_o could decrease more rapidly than E_1 and thus, E_1 would no longer be equal to the peak value of E_o. When T3 is ON, capacitor C1 discharges through R2 and T3 and, on the following cycle of operation, C1 recharges to the new value of E_o. Thus, E_1 is always equal to the peak value of E_o.

Adapt logic circuitry

The Adapt Logic Circuit, shown in Figure 20, is a straightforward arrangement of diode-transistor logic gates. The network connected to the base of T1 realizes equation (1.3) and that connected to the base of T2 realizes equation (1.4). T1 and T2 provide current

gain but their main function is to allow for the adjustment of the increment or decrement pulse height by means of resistors R4 and R8. Let $f_{I_i} = 0$ and $f_{D_i} = 0$. Both T1 and T2 will be held OFF since the bases are near ground potential and the dividers R5 - R6 and R7 - R9 provide sufficient reverse bias. There will be no voltage difference across winding 1 under these conditions. This neglects the flow of I_{c_o} in T1 and T2 but R4 and R8 are so small as to make its effect negligible.

Suppose now that $f_{I_i} = 1$. Transistor T1 will become forward biased and will saturate. The voltage difference across winding 1 becomes

$$E_I = 12 - 12 \left[\frac{R6}{\frac{R4R5}{R4+R5} + R6} \right]$$

and since $R5 \gg R4$

$$E_I \approx 12 \left[1 - \frac{R_6}{R4+R6} \right] \tag{2.2}$$

The amplitude of this increment pulse can be adjusted by varying R4 and R6. However, R6 cannot be too small since the divider R5 - R6 must supply reverse bias and, at the same time, draw as little supply current as possible. In view of these restrictions R5 and R6 were set at 1k and 100 ohms respectively. R4 was then used to control the pulse amplitude. Similarly, the amplitude of the decrement pulse is

$$E_D \approx 12 \left[1 - \frac{R9}{R8 + R9} \right] \tag{2.3}$$

and R8 is used to control the decrement pulse amplitude.

The inductance of winding 1 is nonlinear due to the core, and the design is best done using a graphical method. Figure 21 shows the hysteresis loops for the leg 1 - leg 2 and leg 1 - leg 3 paths. The test frequency was 100 cps and this was considered to provide an approximate value for the switchable flux, $\Phi 2$ and $\Phi 3$, in legs 2 and 3 respectively. Flux $\Phi 2$ is the one which is of interests in the design of winding 1. The present design is such that flux $\Phi 3$ is never switched by the MMF of winding 1. Figure 21 indicates a linear range of about 4×10^{-6} webers. To arrive at a value for $\Delta\Phi$ of equation (1.5) one must decide how many steps are required; that is, one must assign a value to G(n) in equation (1.8). Thus,

$$\Delta\Phi = \frac{4 \times 10^{-6}}{2\,G(n)} \text{ webers}$$

The factor 2 is to account for both the positive and negative portions of the range of the weight.

For example, let G(n) = 25, a_1 = 200 turns and E = 2 volts. Equation (1.5) becomes

$$\tau = \frac{4 \times 10^{-6}}{2 \times 25} \times \frac{200}{2}$$

$$= 8\ \mu s.$$

This is an acceptable value for pulse widths in circuits using germanium devices. Actually, equation (1.5) is misleading in that it represents an ideal case and, one is given the impression that the parameters in the equation can be varied at will in order to arrive at a solution. In practice this was not found to be the case. This point is best illustrated in graphical form.

Consider Figures 22, 23 and 24. Figures 22 and 23 are plots of the relationship between the pulse width, the pulse amplitude

and the maximum obtainable range of operation. The upper limit indicated is the value attained by the peak of the output voltage, E_o of winding 3, for a given pulse-width and pulse amplitude combination. The core was initially returned to the starting position of E_o = 5 volts and then the test pulse was repeatedly applied until there was no further increase in the magnitude of the output voltage. The test circuit used is shown in the diagram. Figure 22 was obtained first using a lower limit of 5 volts. The maximum upper limit for various pulse widths and pulse amplitudes was then found. These curves are referred to as the forward characteristics. The reverse characteristics were found in a similar manner, by selecting 25 volts as the upper limit and decrementing the core until the 5 volt level was reached. The desired range of operation was set from 5 to 25 volts since this range corresponds very closely to the linear portion of $\Phi 2$ as shown in Figure 21. In addition, this sets the total range of the weight at approximately 20 volts.. That is, 2W = 20 volts and hence W = 10 volts. A wider range of operation could be obtained by simply increasing the number of turns on winding 3. However, 25 volts is the maximum rating on the type of transistors used in the equipment.

Going back to the example on page 25, and referring to Figure 22, one can see that, for an initial starting state of 5 volts and the given type of pulse (τ = 8μs, E = 2 volts), the upper limit on the range of operation would be about 11.5 volts. This is not a good solution since the range of operation and the number of steps are both too small. If such a pulse were used to decrease the output, Figure 23 indicates that there would be a negligible decrease from the 25 volt level. This example serves to illustrate the fact that equation (1.5) is insufficient by itself when determining

such parameter as pulse amplitude, pulse width and increment size. It has shown that, due to core imperfections, one must use the graphical data of Figures 22 and 23, in conjunction with equation (1.5), in order to arrive at meaningful values for the above parameters.

It is most convenient to derive the incrementing and decrementing pulse from a common source; hence the pulse width will be the same for both the incrementing and decrementing pulses. To compensate for the assymetry in the core, as demonstrated in Figures 22, 23 and 24, the pulse amplitudes must be adjusted. Resistors R4 and R8 of Figure 20 are adjusted not only to compensate for the mentioned assymetry but to also compensate for variations in characteristics from core to core.

Figure 24 is a plot of the peak value of the output voltage E_o, of winding 3 versus the MMF produced by a direct current in winding 1. The characteristics shown correspond to operation around the major hysteresis loop of the path surrounding aperture 1. The prominent assymetry is characteristic of an incorrectly demagnetized core but various demagnetizing processes did not improve the situation. The conclusion drawn is that more energy is required to move the core from the state shown in Figure 7(c) to the state of 7(a) than is required when moved in the opposite direction. Theoretically, the output should be zero for the blocked state but, due to a squareness ratio of less than unity, there is an output produced even when the core is driven further into saturation. The squareness ratio, as measured on Figure 21, is approximately 0.9.

Figure 22 and 23 may be further analysed to demonstrate an interesting point. Consider a horizontal line drawn through

the characteristic curves of Figure 22. Such a horizontal line corresponds to a specific level of stored flux, which is equivalent to the reversal of flux around aperture 1 out to a specific radius. The points of intersection of this horizontal line, with the existing curves, should all be points of constant pulse width - pulse amplitude product. Figure 25 is a plot of the points of intersection for horizontal lines corresponding to 10, 15, 20 and 25 volts, on Figure 22. As can be seen, the resultant curves are close approximations to the theoretical rectangular hyperbolae. A calculation, based on equation (1.5), has been carried out to determine the maximum number of steps that would result for operation between a lower limit of 5 volts and an upper limit equal to 10, 15, 20 and 25 volts. For example, let the chosen upper limit be 25 volts. We see, from Figure 22 and Figure 25, that one can move from a starting level of 5 volts to a final level of 25 volts through the repeated application of a pulse whose width-amplitude product is approximately 25.6×10^{-6} volt-seconds. Such a pulse is the only one which will give this range of operation.

Equation (1.5) can now be used to calculate the corresponding flux increment. Thus,

$$\Delta\Phi = \frac{E\,\tau}{a_1}$$

$$\Delta\Phi = \frac{25.6 \times 10^{-6}}{200}$$

$$= 12.8 \times 10^{-8} \text{ volt-seconds.}$$

From Figure 21, the flux range corresponding to the 5 to 25 volt range, is seen to be approximately 4×10^{-6} volt-seconds. Thus, the maximum number of steps which can occur over the above range is

$$\text{number of steps} = \frac{4 \times 10^{-6}}{12.8 \times 10^{-8}}$$

$$\approx 32 \text{ steps}$$

The corresponding number of steps were calculated for the other possible upper limits, using the above method.

The characteristics shown in Figure 22 and 23 are due to the finite slope and non-squareness of the hysteresis loop of the core material. Figure 26 shows a more realistic path of operation for the process of flux integration. When compared with the ideal case shown in Figure 8(b), one can see that the resultant flux change, $\Delta\Phi'$; is less than the theoretical value of $\Delta\Phi$. In order to produce a given amount of change in flux one would require a larger E.τ product than is theoretically predicted.

The final parameter values chosen for the Adapt Logic Circuit, and their consequent effect on system operating characteristics, will be discussed in Chapter III.

Input signal buffer

The Input Signal Buffer was included in the design to provide maximum flexibility in the range of input signals. The circuit diagram is shown in Figure 27. This circuit will operate satisfactorily with positive input pulses from 6 to 20 volts, from sources of from 0 to 30k ohms respectively. This range of operation is based on a minimum current gain of 10 for T1 and T2. The transistors are allowed to saturate, since the relatively long input pulse of 200 μs will be little affected.

3. Design of the System Circuits

The design and operation of the system circuits is not one of the topics of this thesis but, a brief discussion of these circuits is given for the sake of clarity and completeness.

Threshold gate and output pulse generator

Figure 19 contains the diagram of the above two circuits. The adding circuit is a grounded base amplifier with a gain of approximately unity and, an input impedance of approximately 40 ohms. This allows the addition or removal of weight units with a minimum of interaction. The threshold level circuit is a Schmitt trigger and preliminary tests on the stability of the upper trip point indicate a range of variation of 0.09 volts; that is, $(\theta_2 + \theta_1)$ of equation (1.12) is equal to 0.09 volts. This value corresponds to a rather narrow temperature range and further testing may be necessary if the equipment is to be operated under widely varying temperature conditions. The Schmitt trigger produces a positive pulse, the width of which varies according to the magnitude of the base voltage of transistor T2. To eliminate possible pulse width variations in the output pulse, Z, the leading edge of the pulse from the Schmitt circuit is used to trigger a monostable multivibrator, which generates a standard, 200μs wide, output pulse.

Increment pulse generator

The Increment Pulse Generator, shown in Figure 28, consists of a trigger amplifier, a monostable multivibrator which generates an adjustable delay signal, an inverting amplifier and another monostable multivibrator, which generates the actual adapt pulse, P. The adjustable delay allows independent positioning of the adapt pulse with respect to the 5kc/s AC signal (see Figure 12). The chosen mode of operation requires that the adapt pulse be applied to winding 1 if necessary, after the weighted sum has been compared with the threshold level. The delay generator provides the required time delay. The position of the adapt pulse with respect to the AC carrier signal, is also important. The adapt pulse must not be applied at the same time that the prime or drive currents are flowing in winding 2. The delay generator thus allows the position of the adapt pulse to be properly set.

Remaining circuitry

The desired signal (D) amplifier and the actual signal (Z) amplifier are identical and the circuit diagram is shown in Figure 29. These amplifiers have been designed to supply ten weight units, the maximum number anticipated. The state of the D and Z variables is indicated on the Display Panel by means of neon bulb indicators, the circuit diagram of which is shown in Figure 30. The circuit of the Training Controls is given in Figure 31.

Photographs of Equipment

Figure 32 is a photograph of the equipment connected for use as a simple pattern recognizer. Only five of the nine input switches and corresponding lamps are used.

Figure 33 shows one of the weight unit cards. The various circuits of Figure 11 are indicated.

CHAPTER III

DESIGN EVALUATION AND TEST RESULTS

1. Individual Weight Characteristics

Five weight units were constructed and were adjusted for the best performance obtainable. Figure 34 shows the operating characteristics, as measured at E_2 on Figure 16, for each of the five units. It was found to be impossible to obtain good results for each weight unit with the same values of components throughout. Resistors R4 and R8 of equations (2.2) and (2.3) had to be adjusted individually for each weight unit to compensate for differences in the magnetic cores. The characteristics shown in Figure 34 were obtained by continuously incrementing the weight unit in the forward direction until saturation was reached and then decrementing the unit until saturation was reached in the reverse direction. The characteristics are reasonably similar and their more important properties are listed, for comparison, in Figure 35. The most obvious defects are the non-linearity of the steps and the saturation regions. Being a magnetic core, the saturation regions are not unexpected. In regard to the nonlinear steps, it has been pointed out by P.R. Low (25) that anomalous hysteresis or big step-little steps effect is shown by all remanent flux storage mechanisms.

On the average, there are approximately 25 steps on the positive or increment slope and 21 steps on the negative or decrement slope. For each weight unit the negative bias was adjusted according to equation (2.1) so that the zero weight value occurred at the midpoint between the upper voltage limit and the lower voltage limit. This resulted in the establishment of approximately 10 to 12 steps over both the positive and negative range of the weight.

In the course of adjusting each of the five weight units, the value of each E_I and E_D was varied and the width of the increment pulse, P, was varied also. The best compromise for the width of P was found to be approximately 20 μs. The width of P was then set at this value and the individual E_I and E_D values were adjusted slightly to give the results shown in Figure 34. Knowing the values of E_I, E_D and τ, one can refer to Figures 22 and 23 to check that the values for the upper and lower voltage limits, obtained from those figures, agrees with the measured values in Figure 35. None of the five sets of data in Figure 35 corresponds exactly to the characteristics shown in Figures 22 and 23 because the core from which these two sets of curves were taken was damaged in subsequent tests and could not be used in a weight units. However, the data in Figure 35 checks reasonably closely with Figures 22 and 23, thus indicating that similar curves apply for each one of the cores in each of the weight units.

Figure 25 and the associated calculations in Chapter II have shown that, for a chosen range of operation of from 5 volts to 25 volts, the maximum obtainable number of steps is approximately 32. This is the maximum number because, the minimum pulse width-pulse amplitude product of 25.6×10^{-6} volt-seconds was used to establish that range of operation. If one attempted to increase the number of steps by reducing either the pulse width or pulse amplitude, the result would be a reduction in the range of operation. Narrower ranges of operation have been shown to contain fewer steps. Thus, for the given core, the maximum number of steps would appear to be close to 32. Figure 35 indicates an average value of 25 steps which is good agreement considering the compromised values of pulse width, τ, and voltages E_D and E_I which were used.

The only remaining point to be discussed is the relationship between results obtained and equation (1.12). Figure 35 provides an estimate of $|W|$ of 9 volts. This was arrived at by averaging the difference between the upper and lower voltage limits (which should, theoretically, be 25 and 5 volts respectively) and dividing by 2 to allow for an equal positive and negative range of values. The quantity $(\theta_2 + \theta_1)$ has been previously measured at 0.09 volts. The factor e, which taken into account variations in w_i due to environental changes and aging of components, is quite difficult to estimate. Temperature coefficient for the switchable flux in the core is -0.3%/ ^{o}C and resistors R1 and R2 of Figure 15 are particularly critical. A safe first estimate for e would be 0.05 to allow a 10 - 15 ^{o}C change in ambient temperature and to provide for other smaller component value changes. Thus, equation (1.12) becomes

$$\frac{9}{G(n)} \gg \Delta w \gg 0.945$$

or approximately

$$\frac{9}{G(n)} \gg \Delta w \gg 1$$

Therefore, G(n) should be no larger than 9. Referring to Winder's table of integral - minimal solutions (Ref (2), page 132), the maximum number of input variables that can be correctly handled is seen to be five, which requires the use of the full range of values from 1 to 9. In view of the nonlinearities it would appear to be safer to set the limit at four variables although, the equipment should correctly realize a fair portion of the functions of five variables. It was this conclusion which led to the reduction of the number of input variables from nine to four. As shown previously, the obtained results were 10 to 12 steps which exceeds the value of 9 just established. Thus, for the case of four inputs, the inability to obtain more steps is not important.

2. Test Results

The following experiments and their results were intended to demonstrate the operation of the weight units when used as adaptive weights in an ATLU. To be completely rigorous, one should test all functions and show that the ATLU does realize the linearly - separable subset. However, for more than two input variables this task would be very lengthy, not only because of the rapidly increasing number of functions but also because of the large number of cycles of adaptation required to reach a solution for any one of the functions (infinite for a non-separable function). Consequently, the following simple tests were carried out in the hope that they constituted an acceptable compromise.

Two-input case

A total of three weight units were placed in the ATLU system (Figure 10), one for each of the input variables x_1 and x_2 and, one for the threshold weight, w_3. Figure 36 contains the data for the complete testing of all 16 Boolean functions. In each function the test procedure was as follows:

1. x_1, x_2 and x_3 were set to 0 and the machine was placed in the ERASE mode. This set the initial values of all weights at the largest possible negative value.

2. With the machine in the OPERATE mode, each input combination was applied, working down from the top. If a particular input did not map correctly, the machine was placed in the ADAPT mode and the error was automatically corrected.

3. After such a correction, the sequence of testing reverted to the top of the column to ensure that previously correct responses had not changed.

4. This procedure continued until the function mapped correctly or an obvious oscillation of weight values was noticed, as in the case of the non-separable functions.

5. The number of required adaptations was noted for each function.

No difficulty was experienced in realizing the 14 separable functions.

Three-input case

Another weight was added to the system to provide three inputs. No attempt was made to check all functions but instead, a number of functions were chosen at random and checked for linear separability. The chosen functions are listed in Figure 37 and the previous training procedure was used. Some of the functions chosen for testing were not threshold functions and are marked with an asterisk. Figure 38 shows the three-dimensional representation of these functions.

Functions 2 and 4 are obviously non-realizable. Functions 0 and 1 should be realizable but are not, due to some fault in the system. It is the belief of the author that the nonlinearity and rather large steps over the linear region of weight are the causes of the trouble. However, given a different starting condition and a different adaptive procedure, it is possible that the given system might be able to realize the functions in question.

Four-input case

With the addition of a fourth input it was decided that instead of attempting the realization of a selection of functions, that the four inputs would be considered as a four-point input matrix. Thus, very simple pattern classification tests could be performed. One advantage

of such tests was the relaxation of the demands on the equipment; that is, it would no longer be necessary to be concerned with completely specified functions but instead, there would be a considerable number of "don't cares" in the function truth tables. Also, there has been considerable interest shown for such equipment used as pattern recognizers. Figure 39 shows the small number of pattern tested. In each case, the conjugate mapping was also carried out.

The adaptive procedure used was as follows:

1. The memory was erased prior to presenting any patterns.

2. The patterns to map as 1 were presented in order until all mapped correctly.

3. The pattern to map to 0 were presented in order until all mapped correctly.

4. The previous mappings were checked and corrected if necessary.

5. The procedure was repeated until correct mapping of all inputs occurred or an obvious oscillation of weight values indicated a non-realizable function. No attempt was made to measure convergence times or best methods of adaptation. The only purpose of the tests was to illustrate the basic capabilities of the weight units.

The foregoing series of tests could be made much more complicated, as there are endless varieties of adaptation schemes, input sequences and initial starting condition which could be used. However, as previously mentioned, the main purpose of the work was the development of an adaptive weight unit and not the study of the operating characteristics of a system of such units.

3. Conclusions

The most obvious conclusion to be drawn concerning the weight unit is that it is not a very good one, at least not as far as the majority of the requirements listed in Section 3 of Chapter I is concerned. The only items in that list which are met by the developed weight unit are items number 2, 3, 4 and 8. The cost is approximately $15.00 per unit, which is a moderate price compared to some other types of weight units. The most objectional shortcomings concern items 5 and 6. These properties would have to be improved upon if one was to seriously consider the use of a large number of these weight units.

The operating range obtained, and the number and linearity of the steps over that range, also leaves much to be desired. However, it has been shown that, for the given core, close to the best possible results have been obtained. There may conceivably be applications where a multi-level storage device, with properties similar to those of this weight unit, would be useful. In fact, this would appear to be the most logical use for the device, at least in its present form. If one desires to go beyond four input variables when using the weight units in an ATLU, then it is advisable to improve the weight unit by way of a core re-design. More data concerning transfluxors is now available as are numerous commercial transfluxor devices.

The development work of this thesis has adequately shown the great differences that can exist between the theoretical concept of how a device should work and how the actual, physical device does work. The imperfect hysteresis curve of the core is the main cause of these differences.

Until just recently the workers in the field of threshold logic and adaptive pattern recognition, have neglected the very

practical problems of stability and component tolerance. The conclusion now being drawn by these people is that the only hope for the practical use of threshold logic, and adaptive pattern recognizers, which have large numbers of inputs (>6), is the decomposition of the large input gates into multi-level arrangements of many simpler gates each having only a few inputs. For example, Mays (26) has stated that for a TLU to handle all functions of 50 variables would requires a component stability of 0.000001%. Fifty inputs is not an excessively large number in the case of pattern recognition. In addition, if many, simpler gates are to be used, then the gates and adaptive weight must be small, simple and inexpensive. The weight unit developed in the course of this work certainly does not fall into such a category, at least not in its present form.

A conclusion of general application can be drawn from equation (1.12) which would apply to systems which have the same automatic adaptive procedure as in the present machine. If $(\theta_1 \pm \theta_2)$ is made very small, then we may write

$$\frac{W}{G(n)} = 2e\,|W|$$

as the limiting case and

$$G(n) = \frac{1}{2e}$$

Thus, it would appear that such a process of automatic adaptation is only applicable for small G(n) and hence, for circuits with small numbers of input variables. For example, e = 0.01 is a practical, economic, lower limit and gives G(n) = 50. With the present amount of information (19) this would correspond to the group of Boolean functions

with up to seven or eight input variables.

The development of adaptive weights with large numbers of steps appears senseless, since one is always limited by component tolerances and stabilities in the order of 1% or 0.1%, at the best. Decomposition appears to be one answer to the problem and once adaptive procedures for such multi-level networks are discovered, then crude weight units such as the one herein described, may perhaps assume some importance.

FIGURES

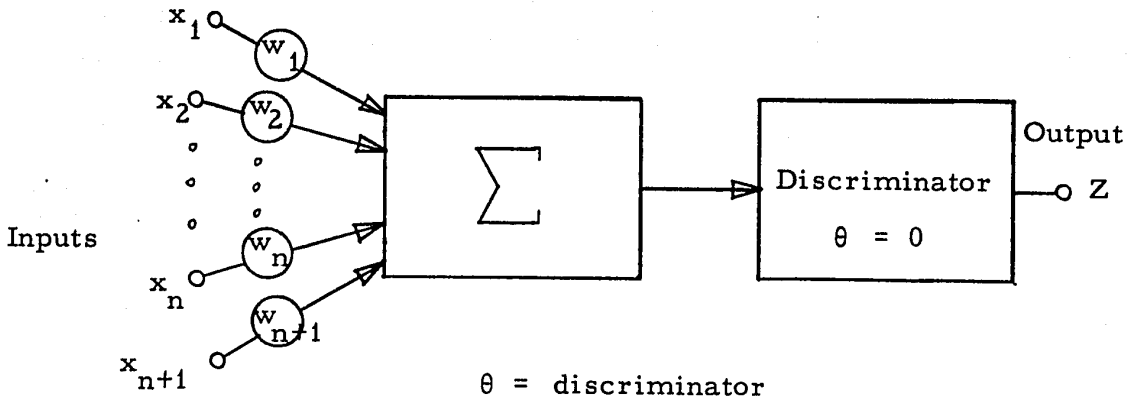

Figure 1. Threshold Logic Unit.

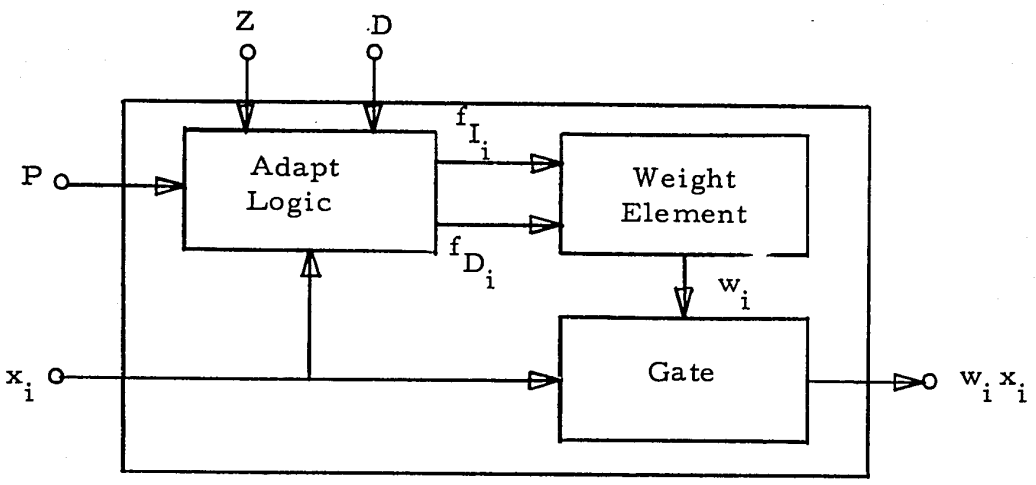

Z - actual output of ATLU.

D - desired output of ATLU (supplied by the operator during training.)

P - adapt pulse whose width (τ) and amplitude (E) control the size of the increment in w_i.

f_{I_i} - function controlling the increase in w_i.

f_{D_i} - function controlling the decrease in w_i.

Figure 2. Adaptive Weight.

P	Z	D	x_i	f_{I_i}	f_{D_i}
1	0	0	0	0	0
1	0	0	1	0	0
1	0	1	0	0	1
1	0	1	1	1	0
1	1	0	0	1	0
1	1	0	1	0	1
1	1	1	0	0	0
1	1	1	1	0	0

Figure 3. Adapt Logic Truth Table.

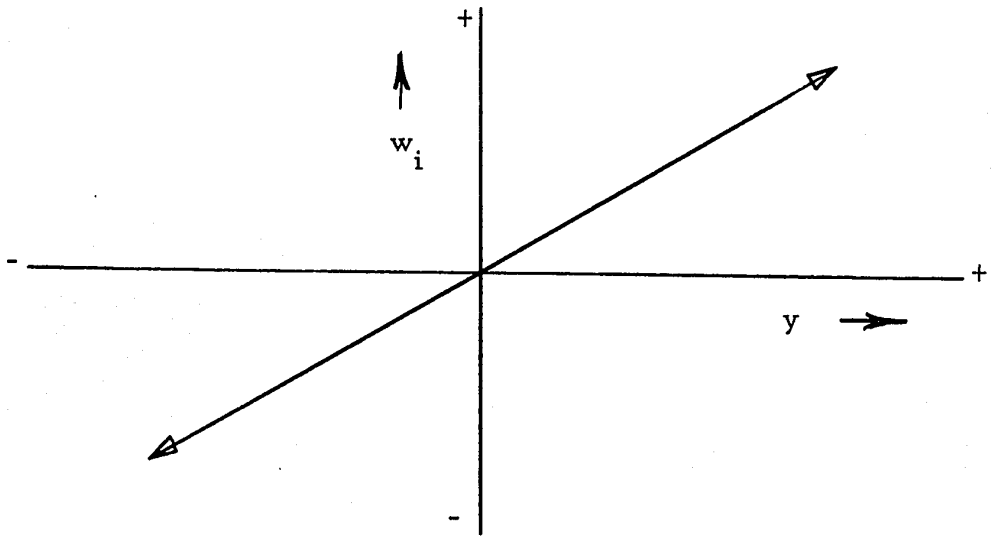

Figure 4. Ideal Weight Characteristic.

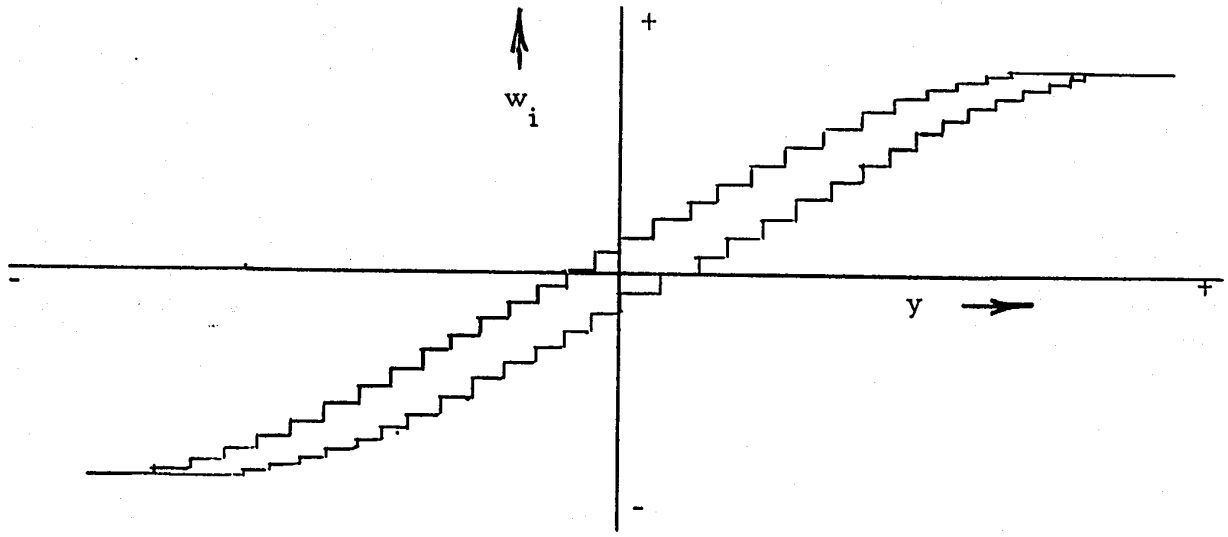

Figure 5. A Possible Actual Weight Characeristic.

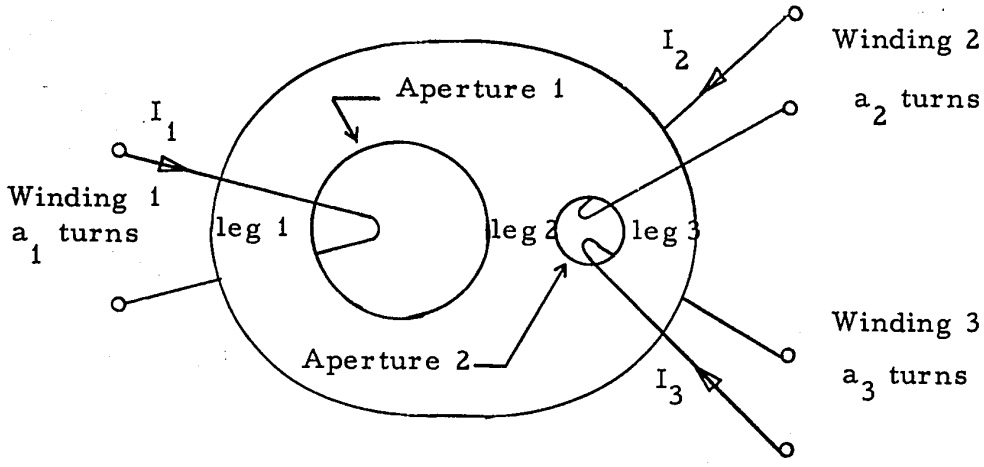

Figure 6. Transfluxor Diagram.

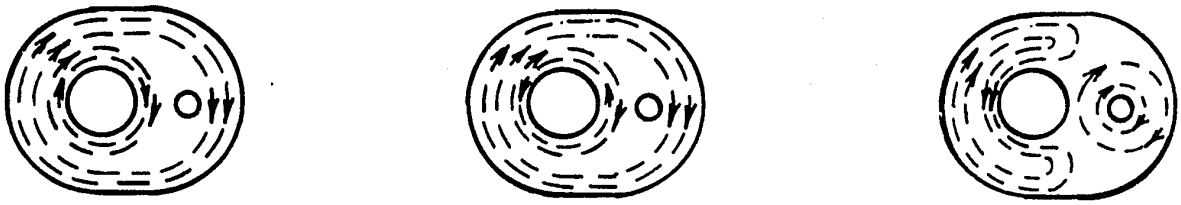

(a) Blocked

(b) Partially Unblocked

(c) Completely Unblocked.

Figure 7. Various Transfluxor States.

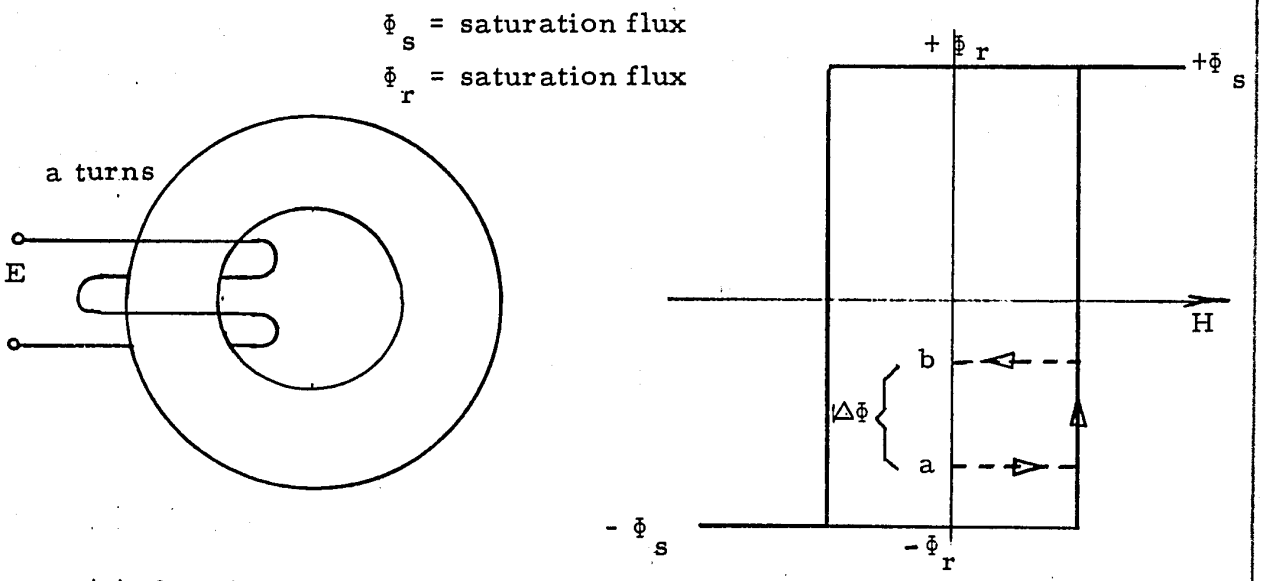

(a) Simple toroid

(b) Hysteresis loop

Figure 8. Flux Integration Process.

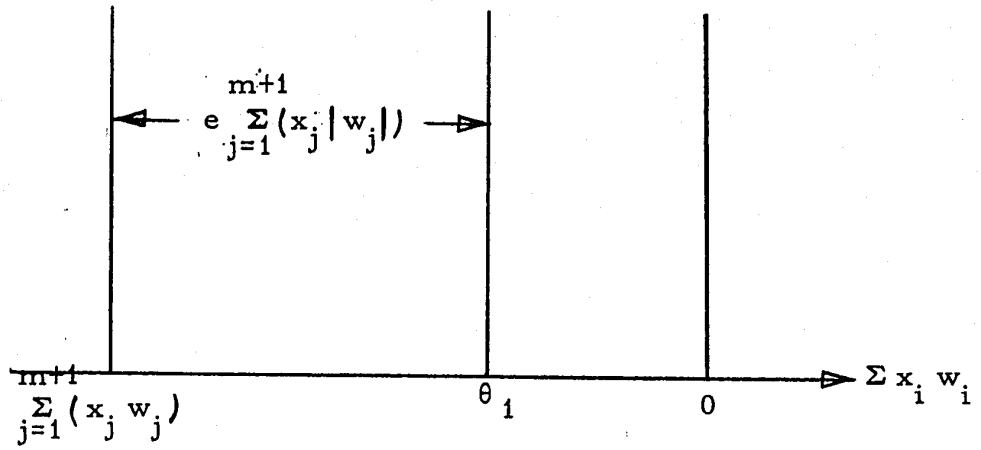

(a) Case 1.

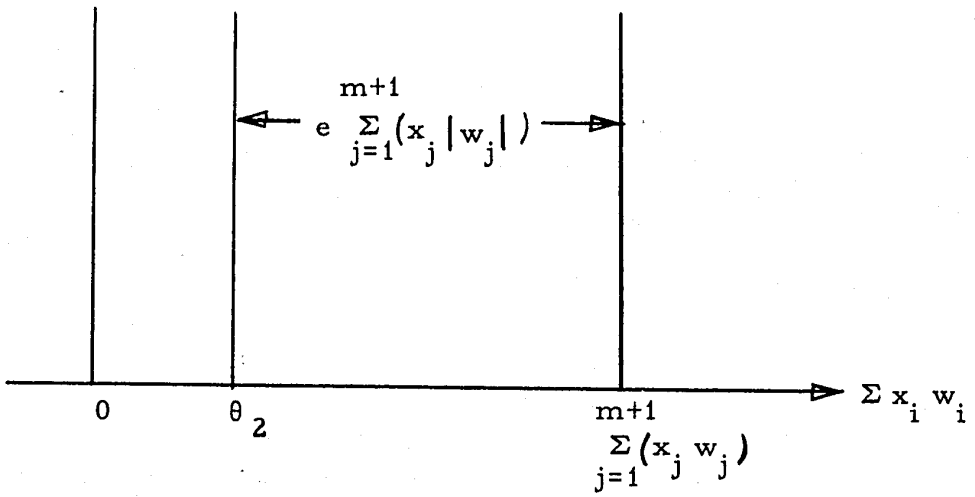

(b) Case 2.

Figure 9. Diagram of Weighted Sum.

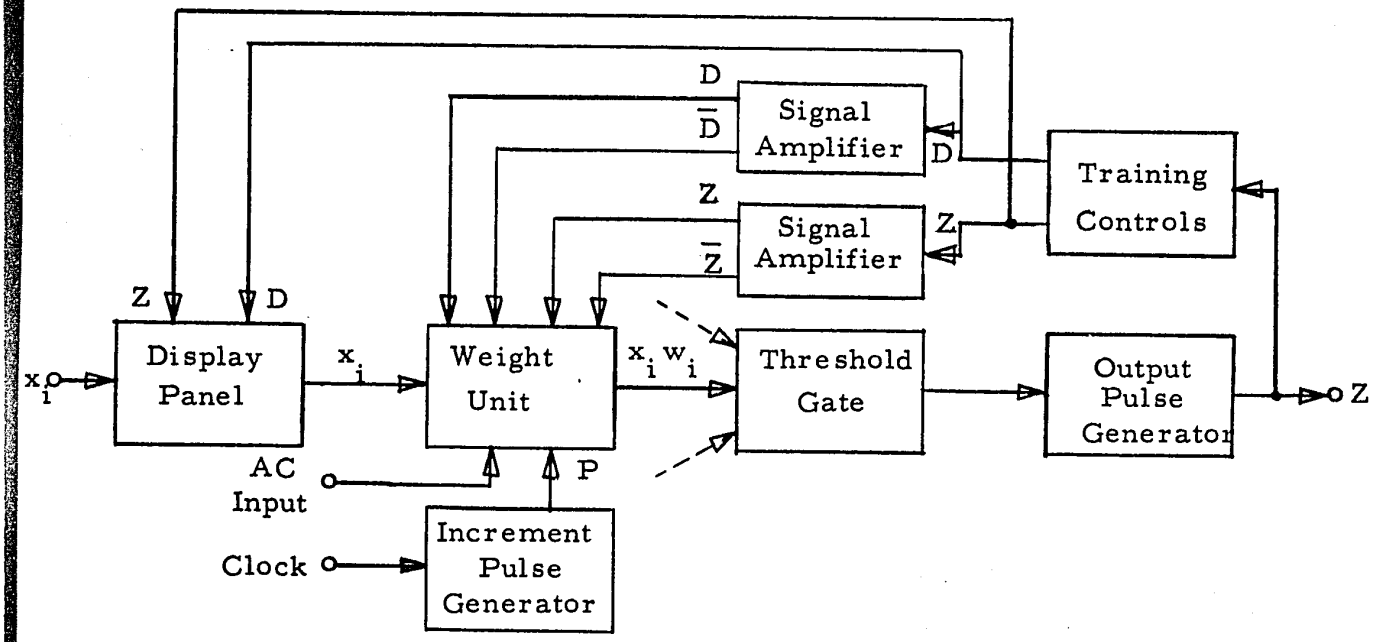

Figure 10. System Block Diagram.

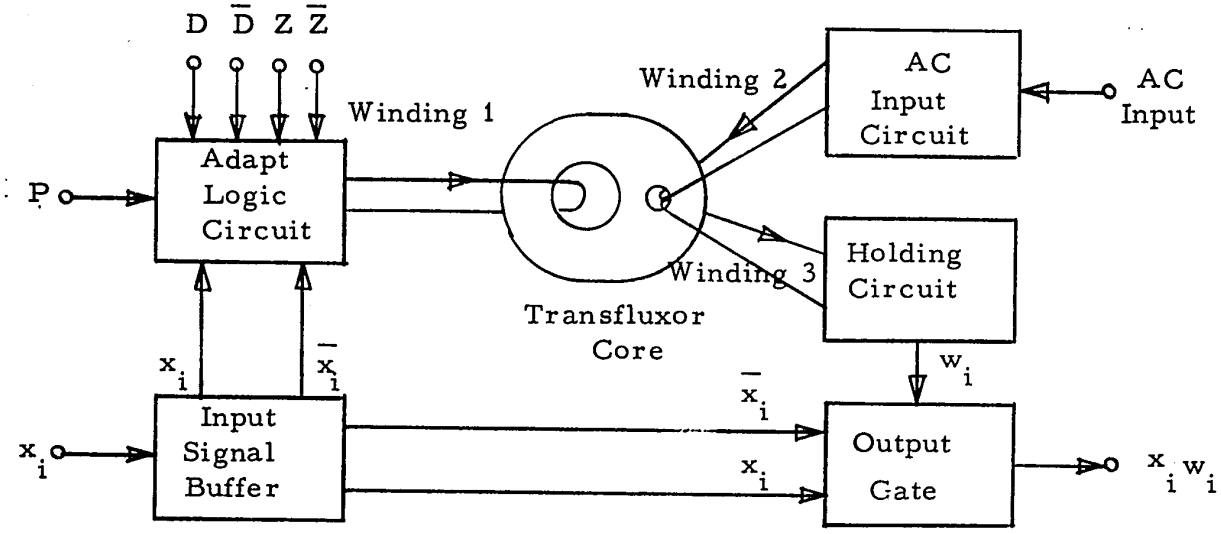

Figure 11. Weight Unit Block Diagram.

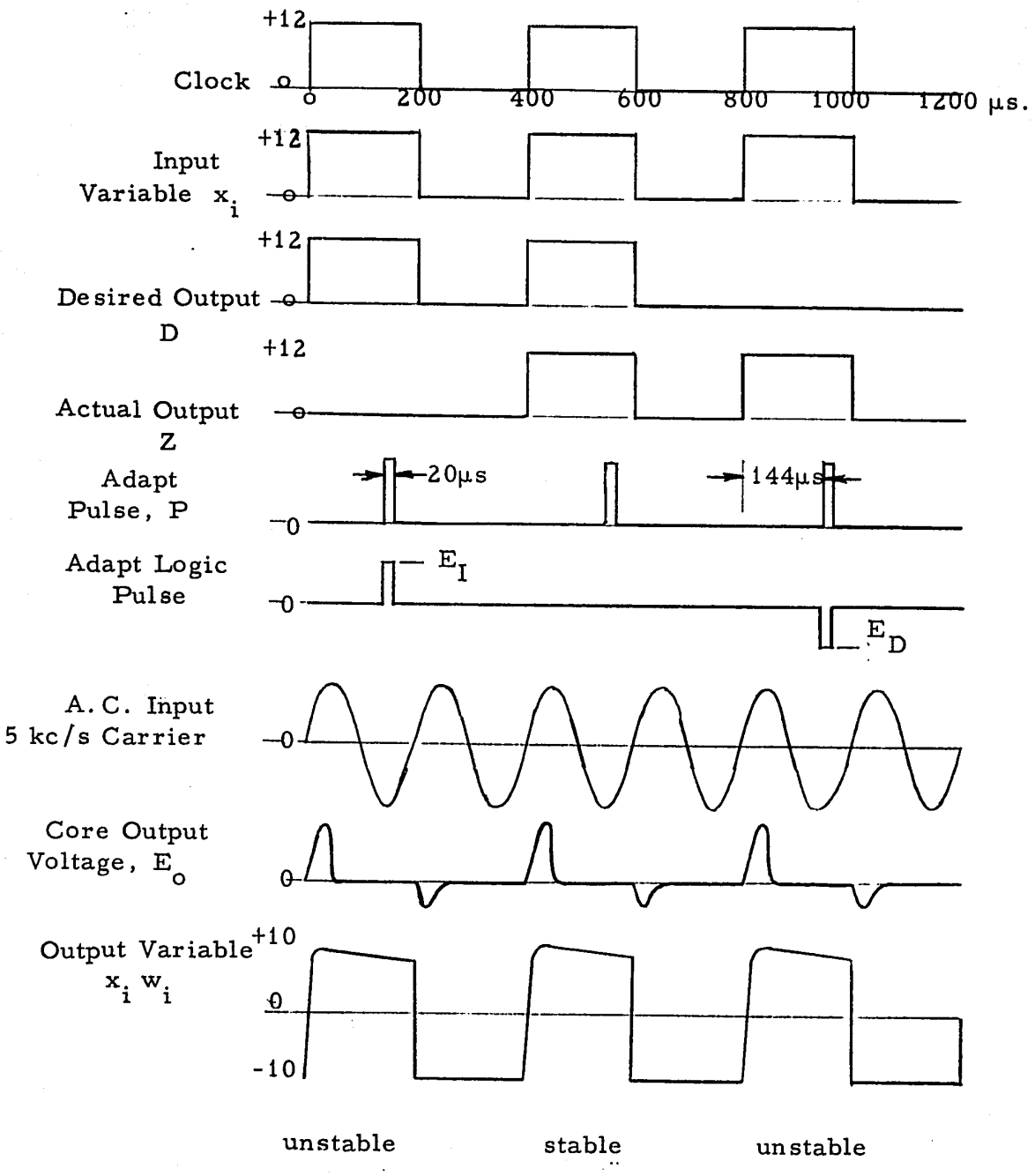

Figure 12. Signal Time Diagram for Three Typical Cycles of Operation.

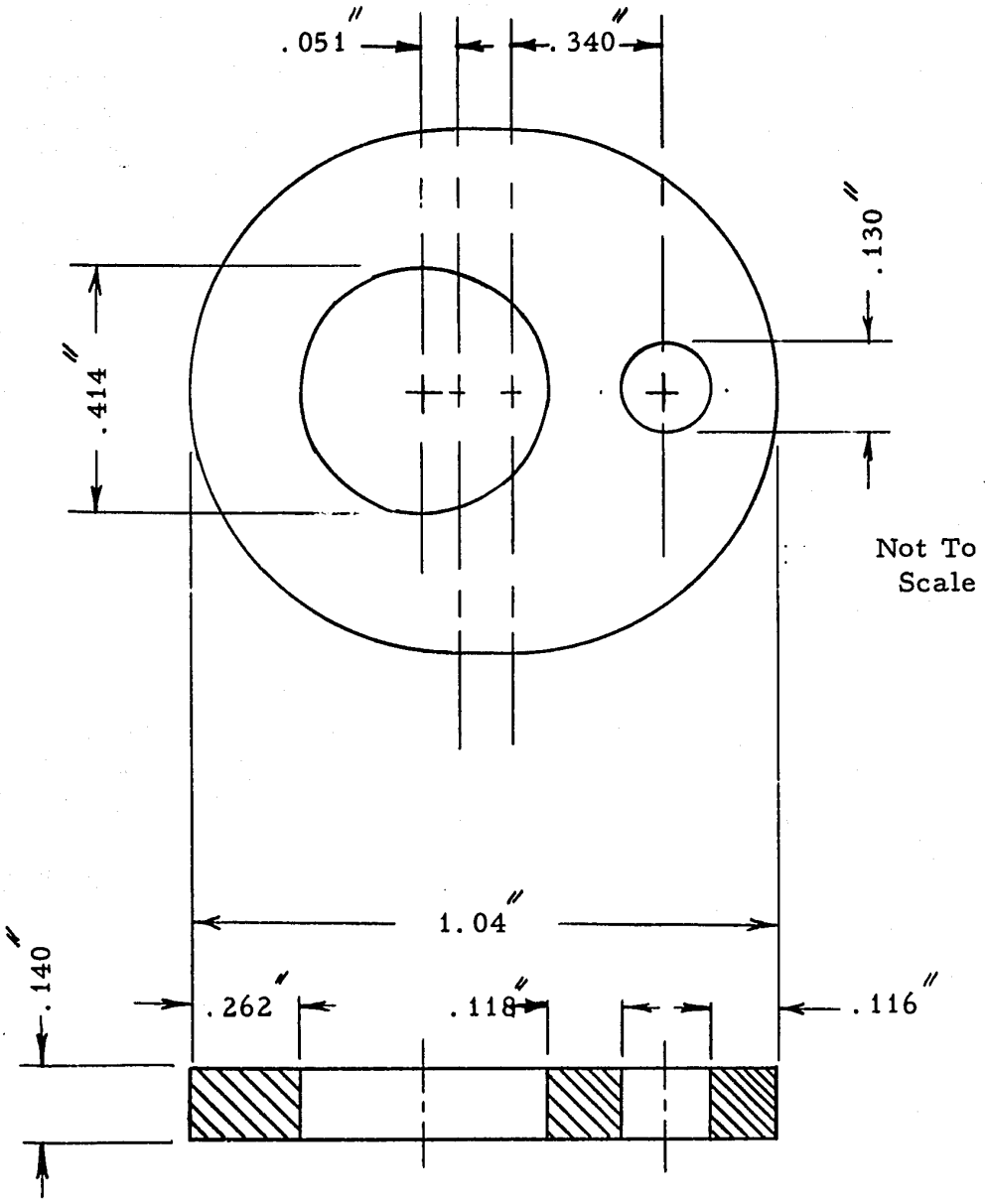

Figure 13 - Physical Dimensions of Core.

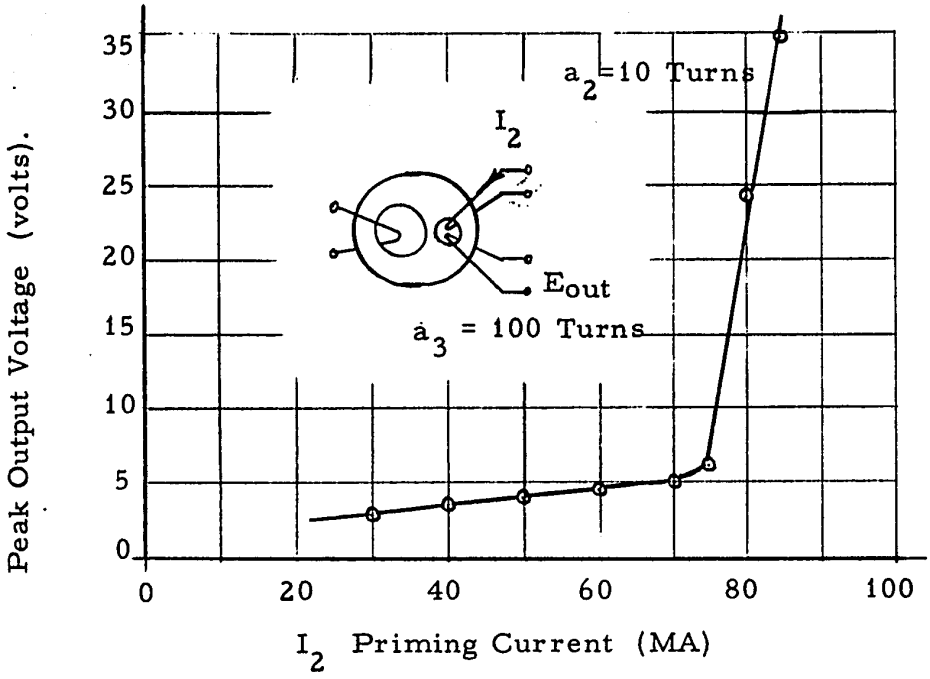

Figure 14 - Peak Amplitude of Output Voltage vs Priming Current for the Blocked State.

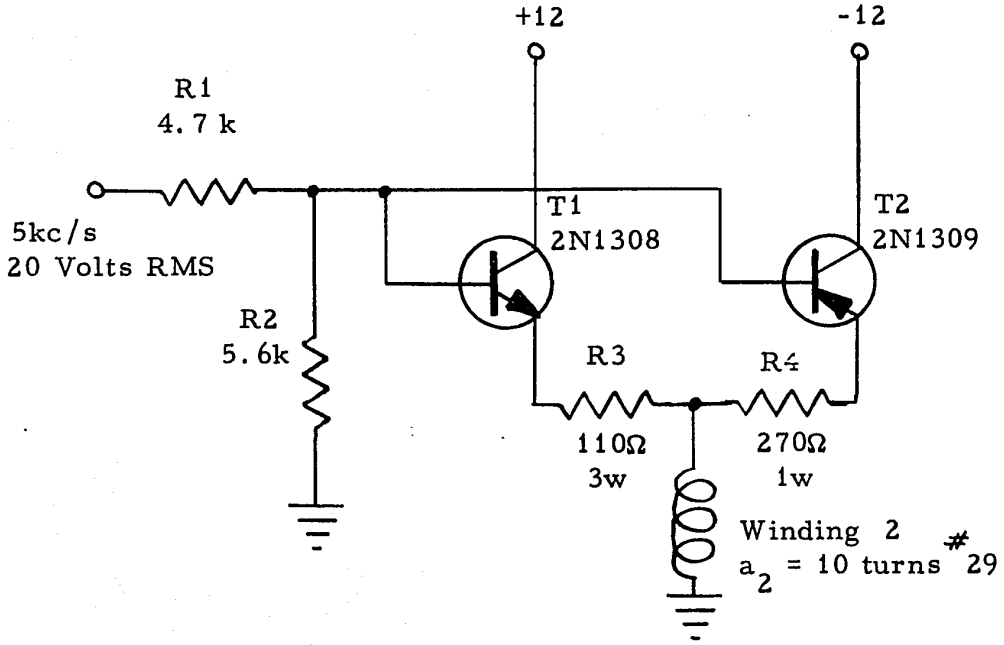

Figure 15. AC Input Circuit.

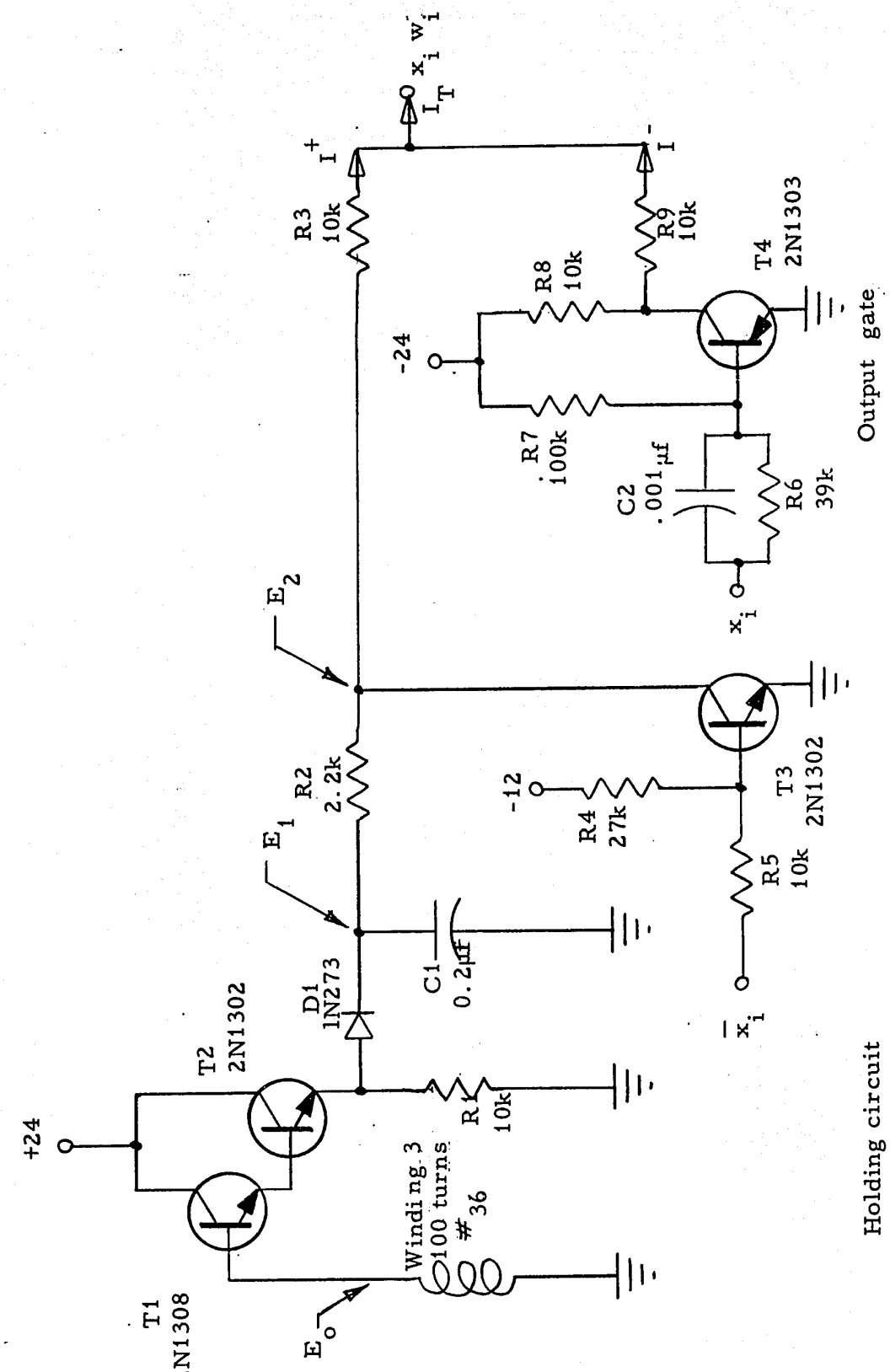

Figure 16. Holding Circuit and Output Gate.

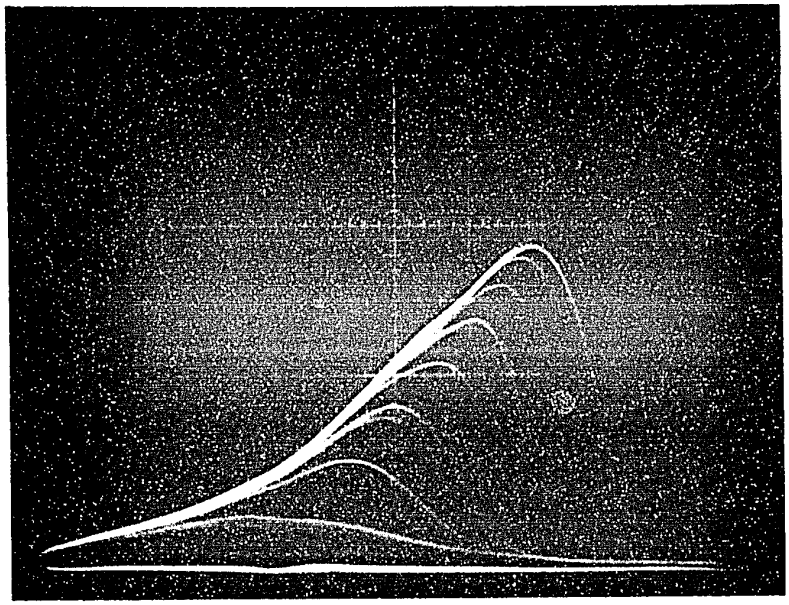

Vertical scale: 5 volts/div Horizontal scale: 2μs/div

Figure 17

Time Shift of Peak Output for Stored Levels Between Maximum and Minimum Stored Level.

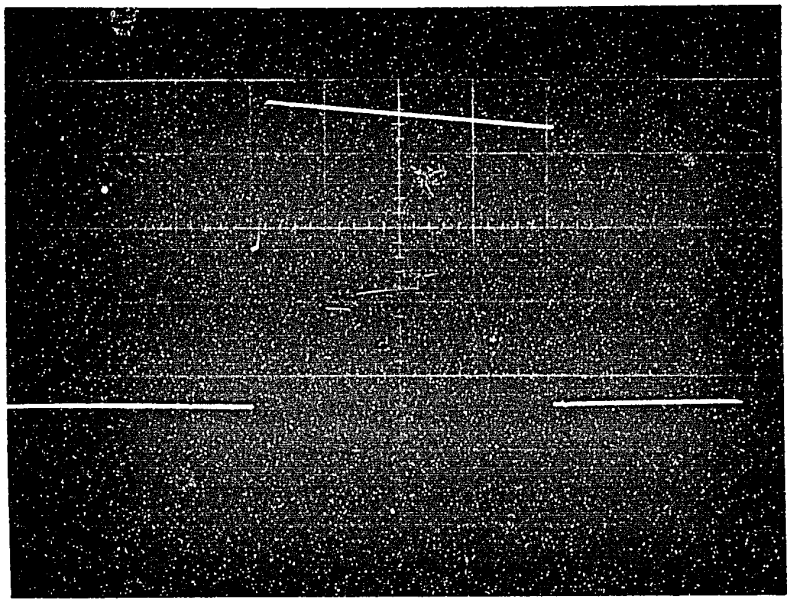

Vertical scale: 5 volts/div Horizontal scale: 50μs/div

Figure 18

Typical Output Pulse Representing the Product $w_i x_i$.

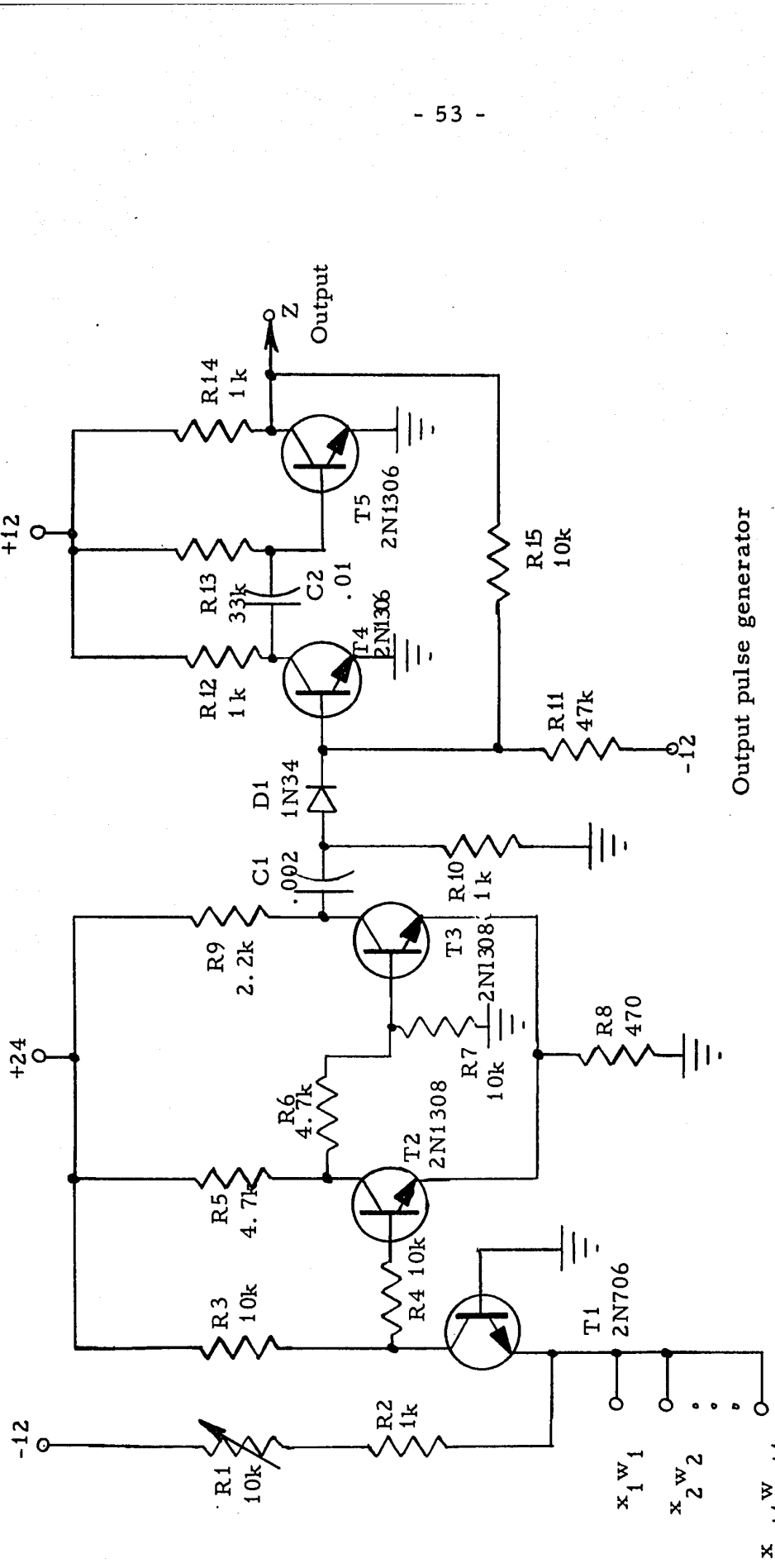

Figure 19. Threshold Gate and Output Pulse Generator.

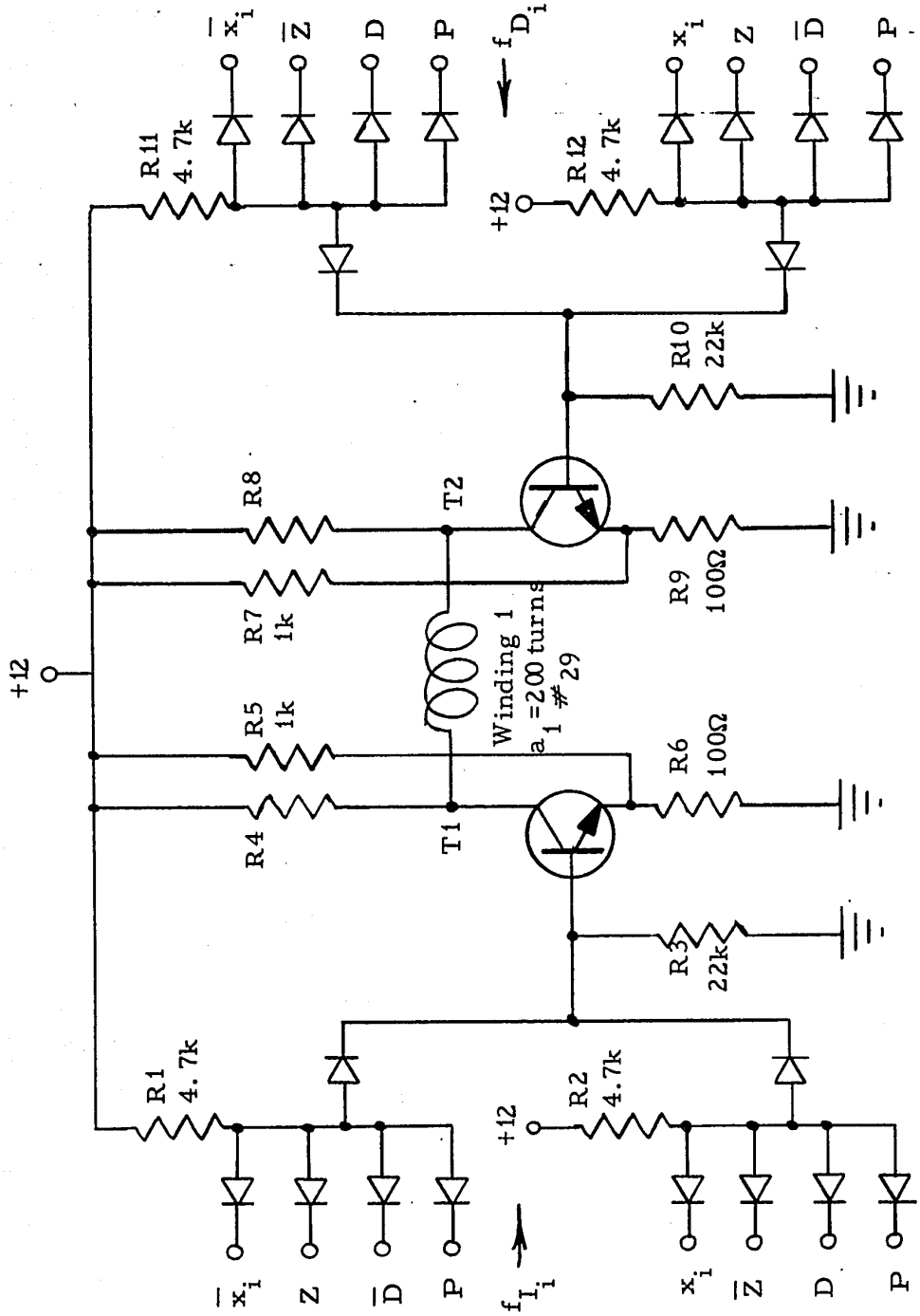

Diodes - 1N34
Transistors - 2N1308
R4, R8 - Set by trial to values between 33 and 56 ohms.

Figure 20. Adapt Logic Diagram.

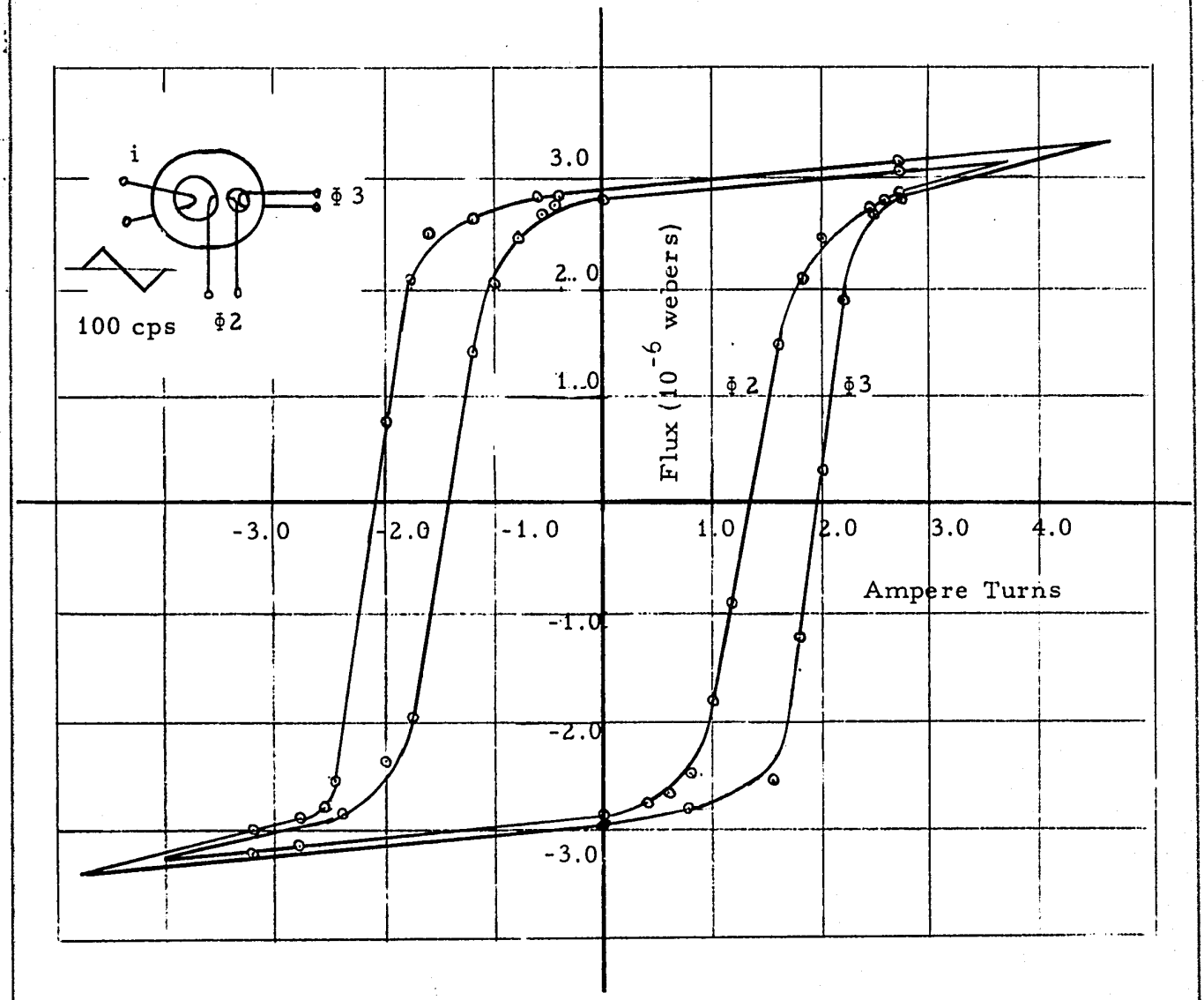

Figure 21. Hysteresis Loop

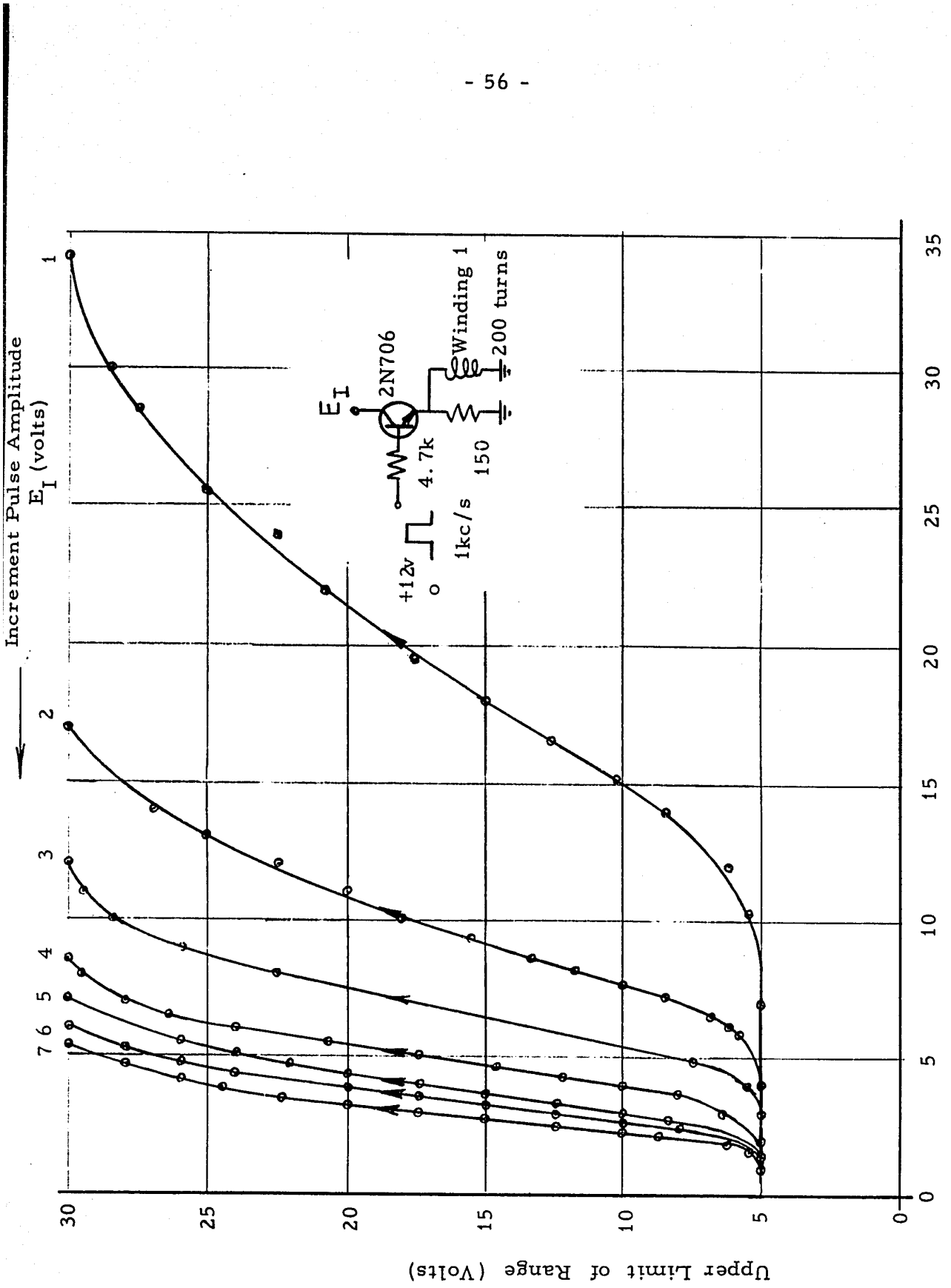

Figure 22. Pulse Width - Pulse Amplitude - Range Relationships (Forward Direction)

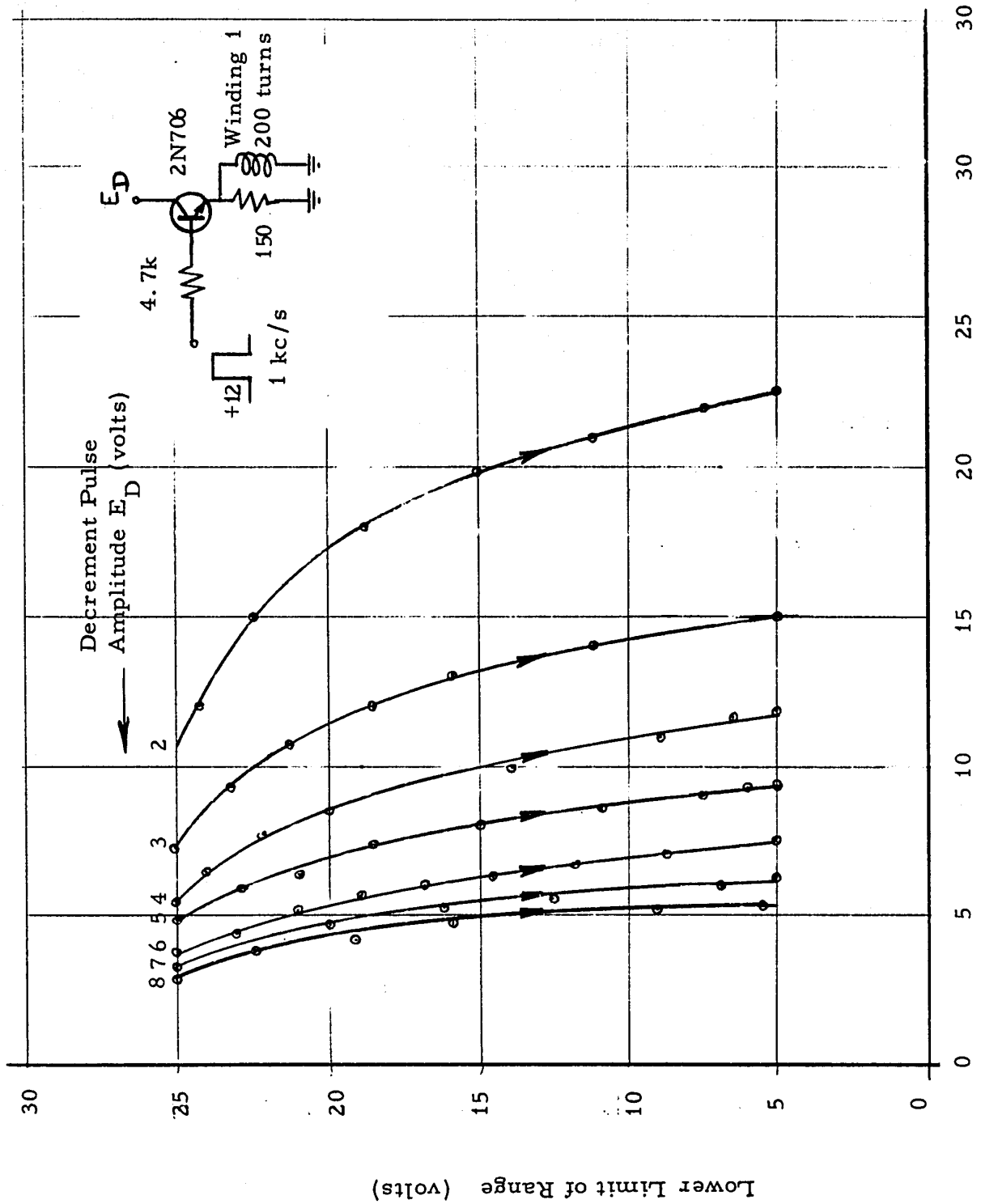

Figure 23. Pulse Width - Pulse Amplitude - Range Relationships (Reverse Direction)

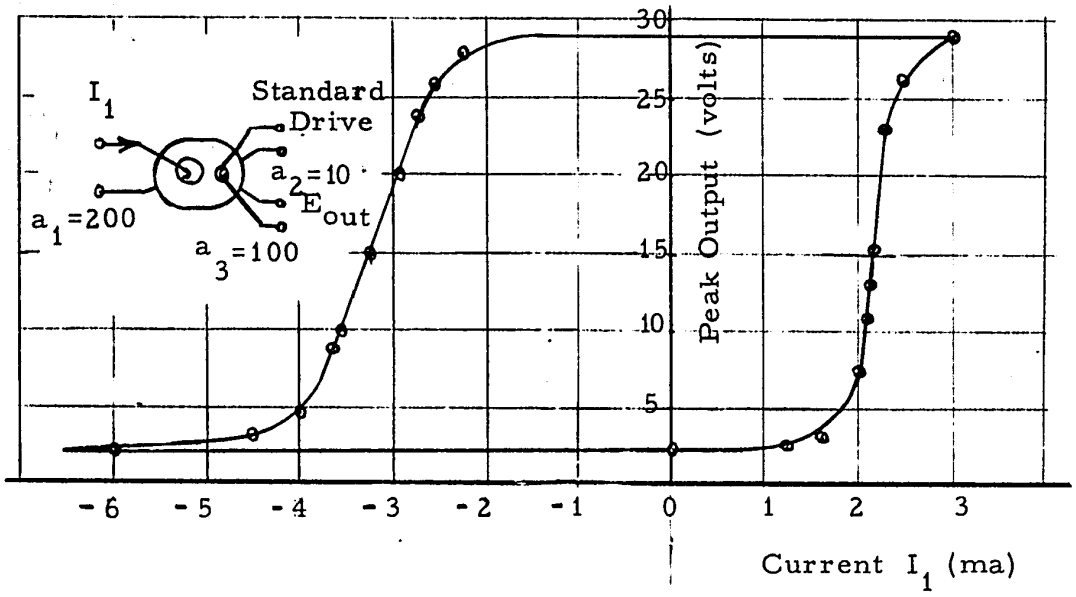

Figure 24. Peak Value of E_{out} vs I_1

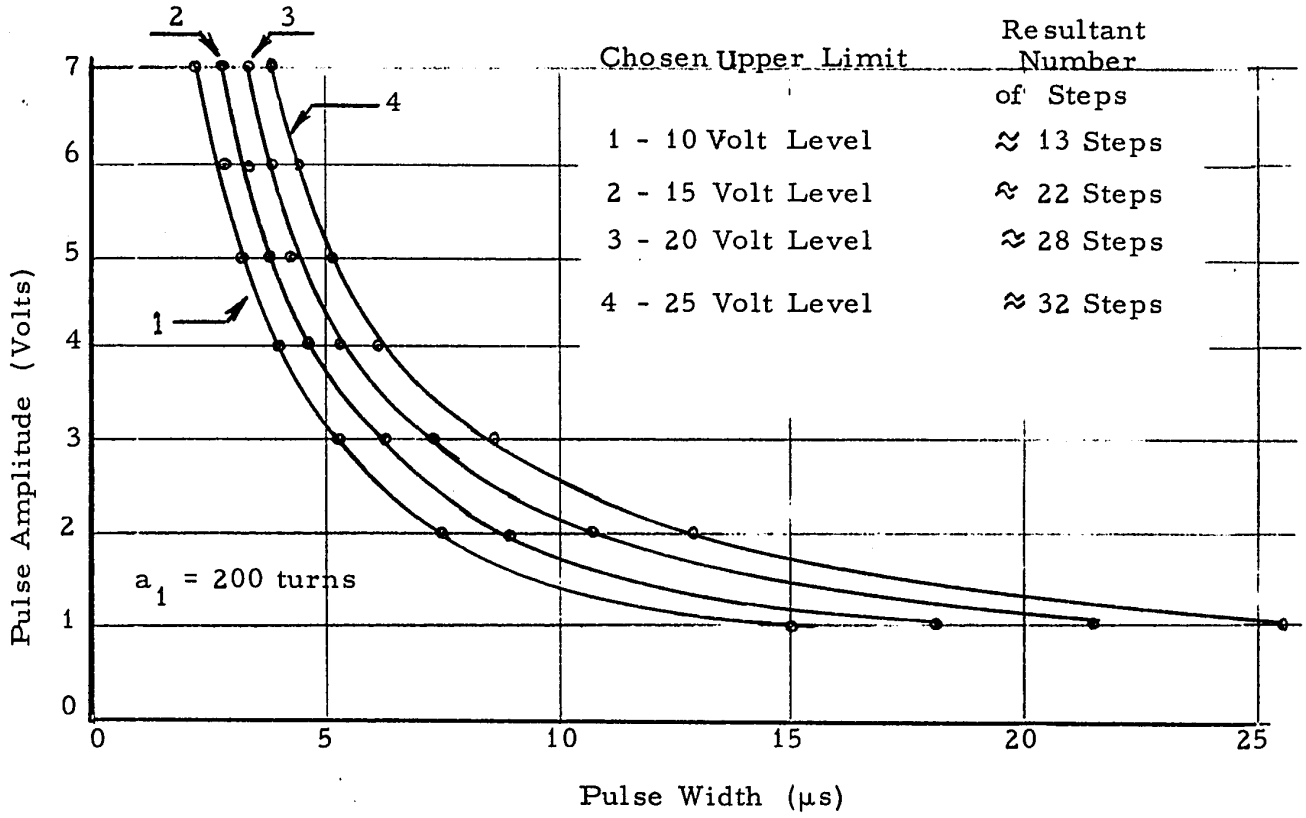

Figure 25. Pulse Width - Pulse Amplitude Relations.

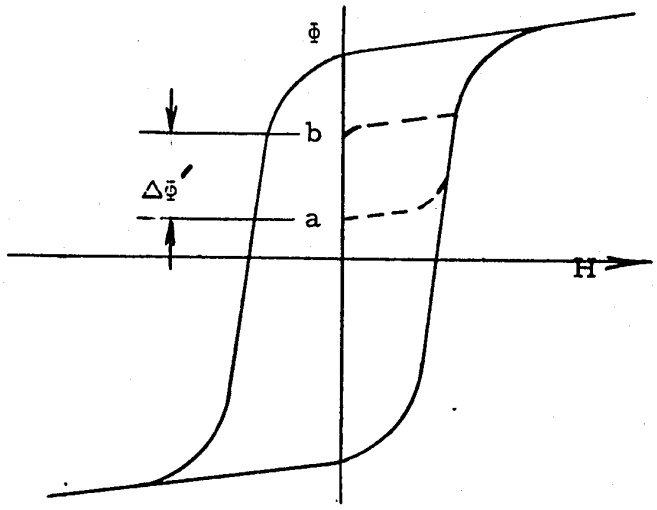

Figure 26. Actual Flux Integration Path.

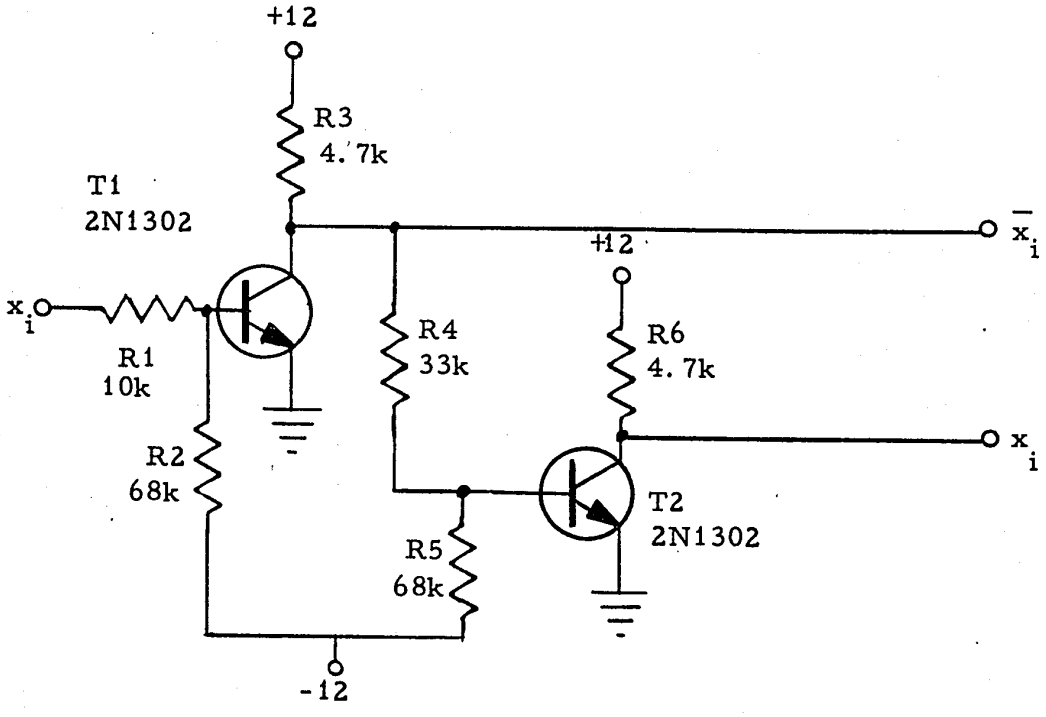

Figure 27. Input Signal Buffer Amplifier.

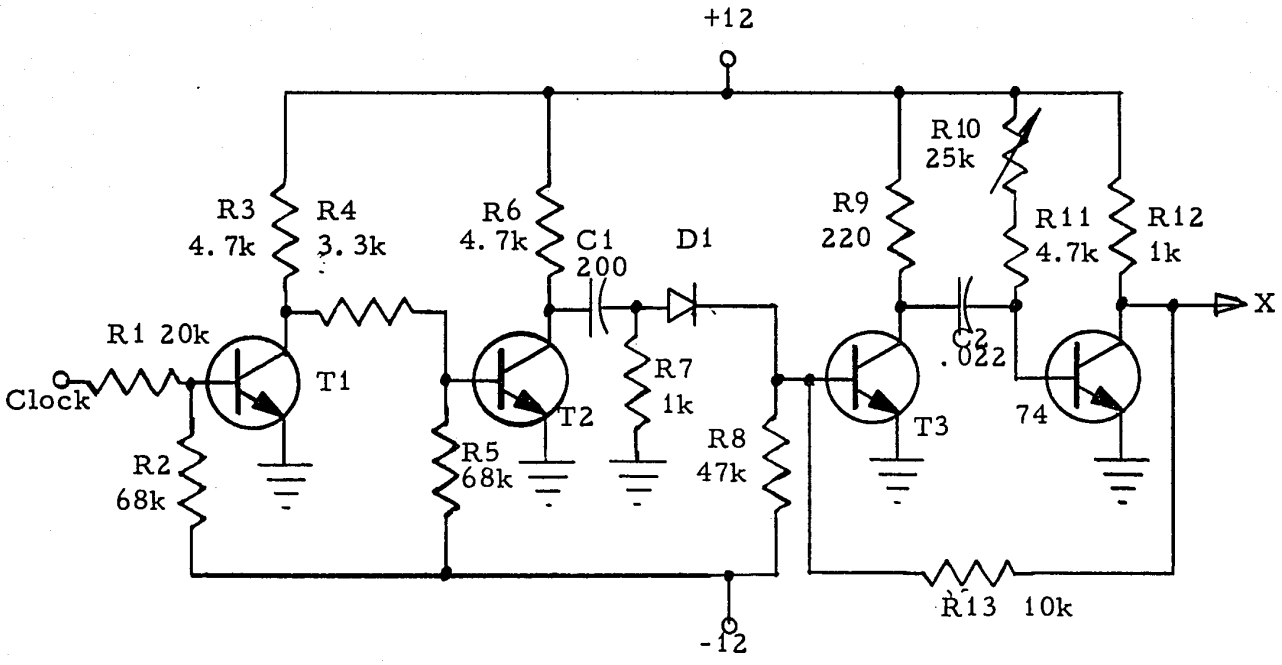

Trigger amplifier and delay generator

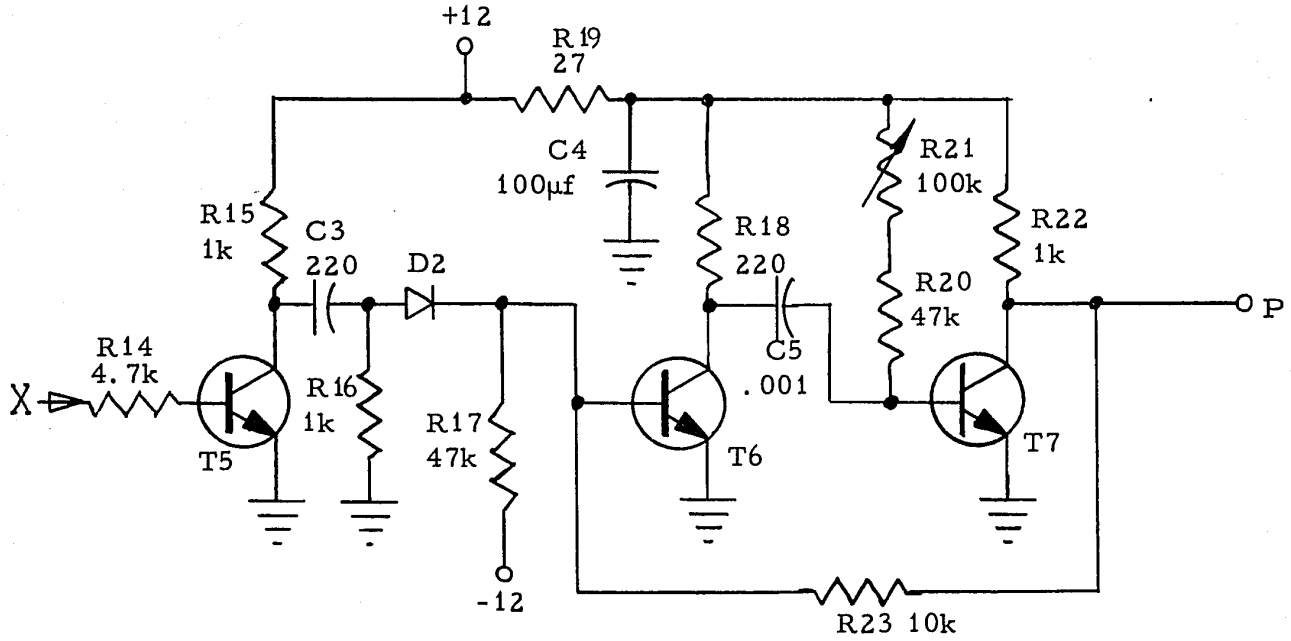

Inverting amplifier and pulse generator
All transistors - 2N706
All diodes - 1N34

Figure 28. Increment Pulse Generator.

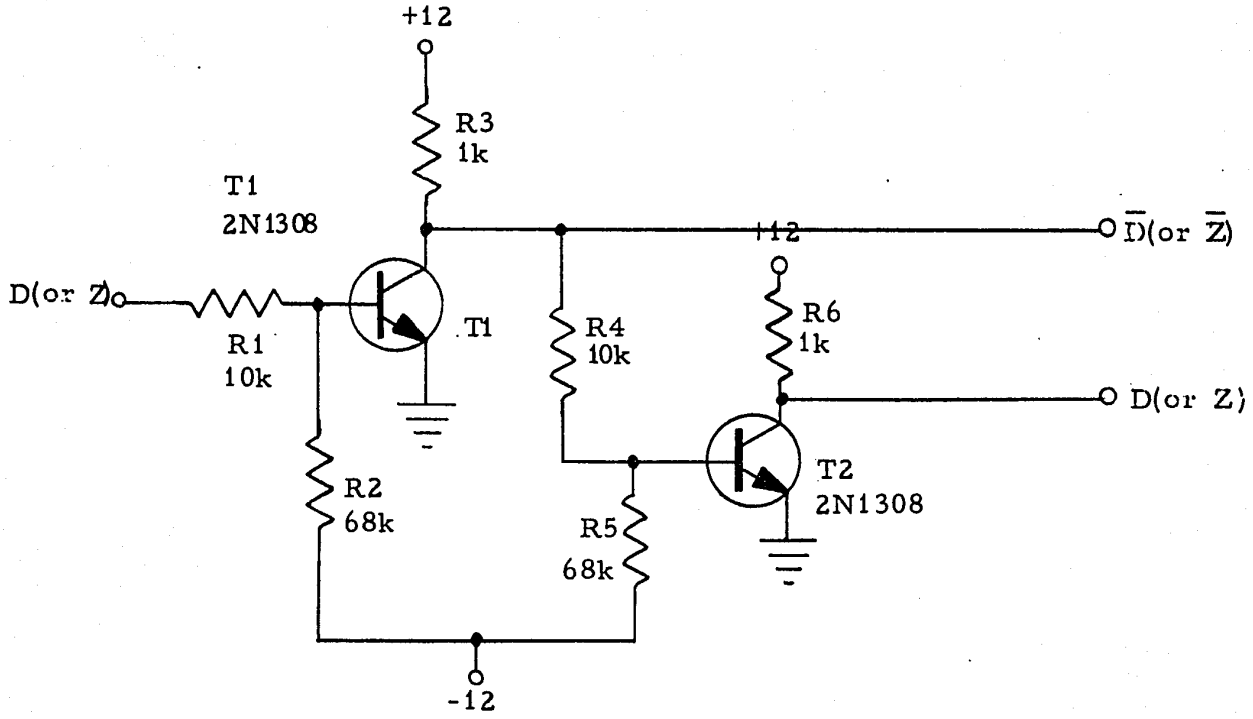

Figure 29. Signal Amplifiers

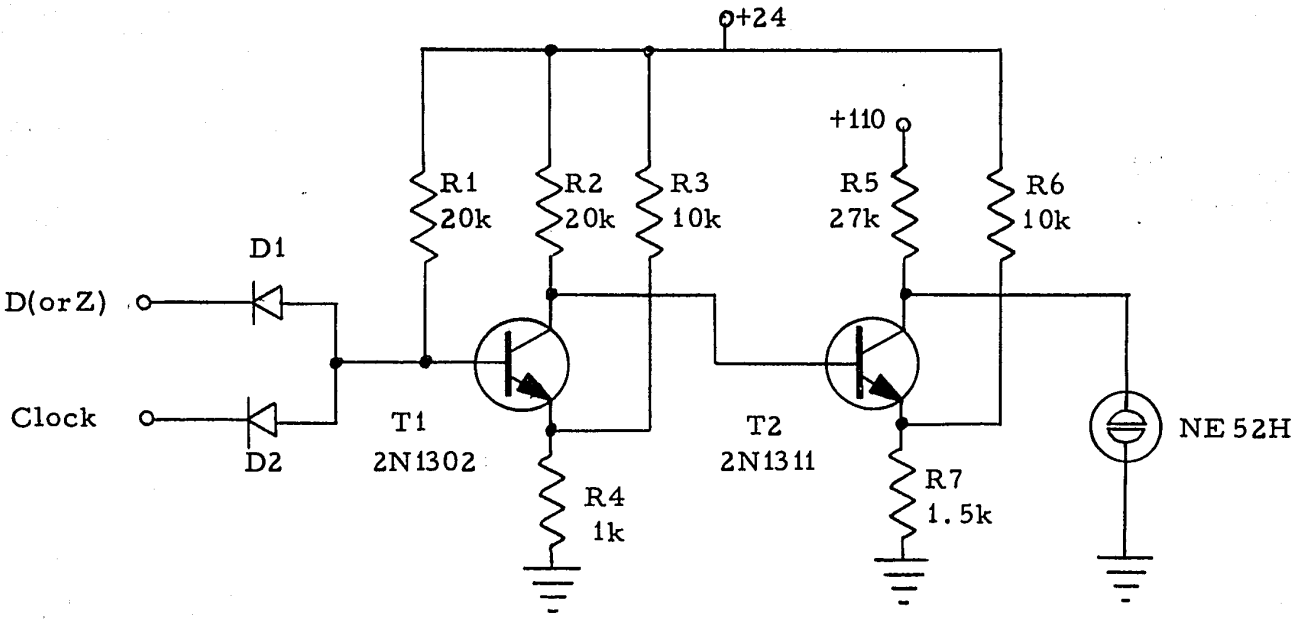

Figure 30. Display Panel Indicator.

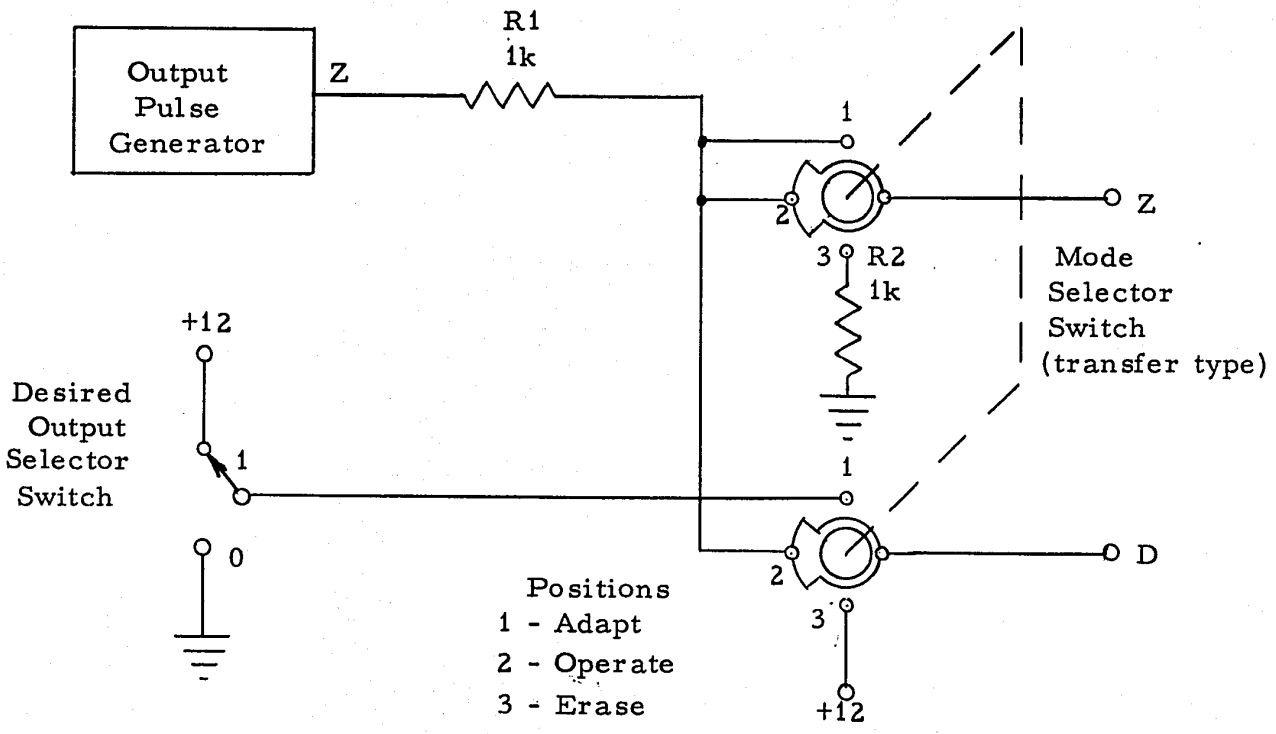

Figure 31. Training Controls.

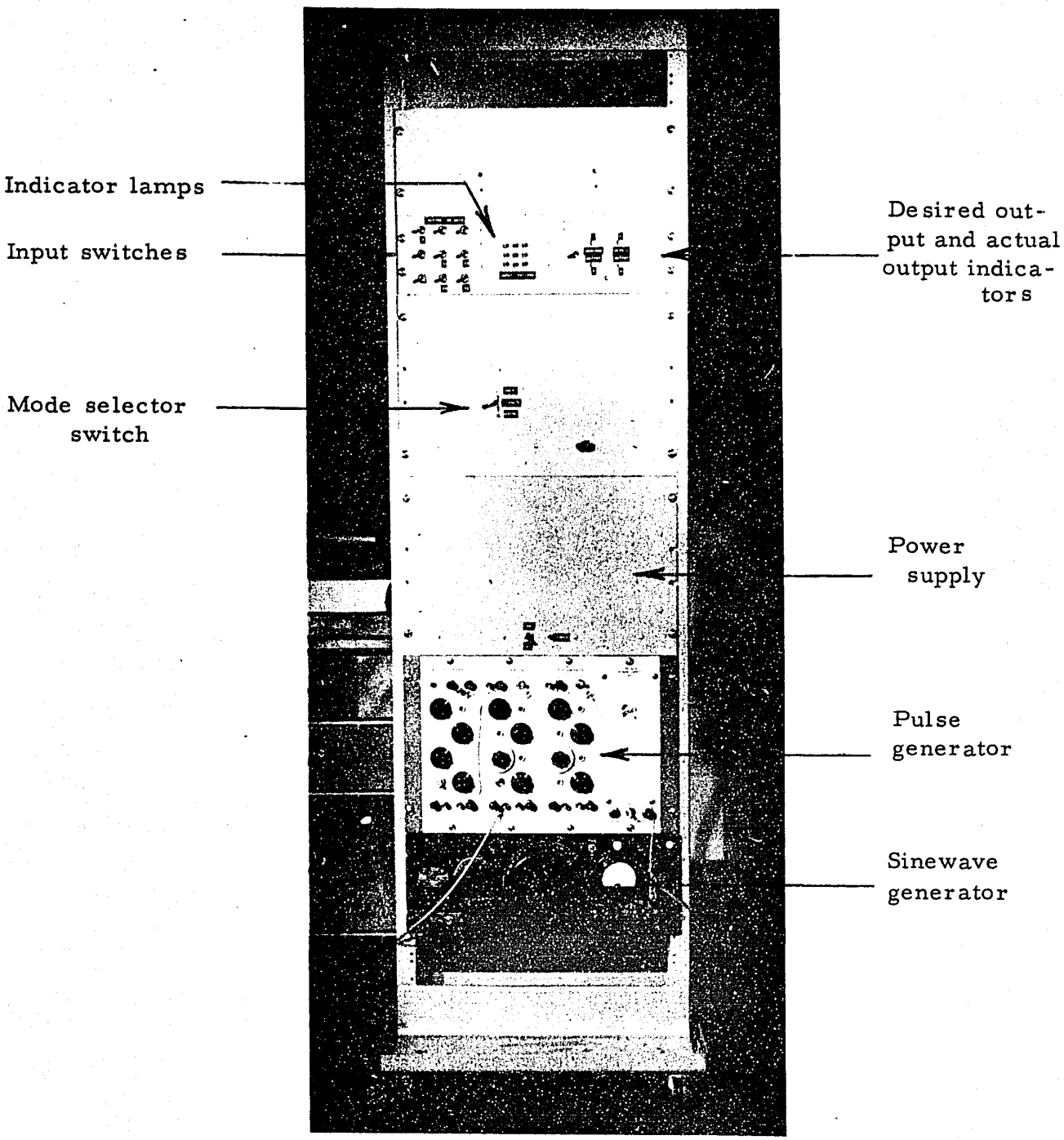

Figure 32
Adaptive Threshold Logic Unit and Associated Equipment.

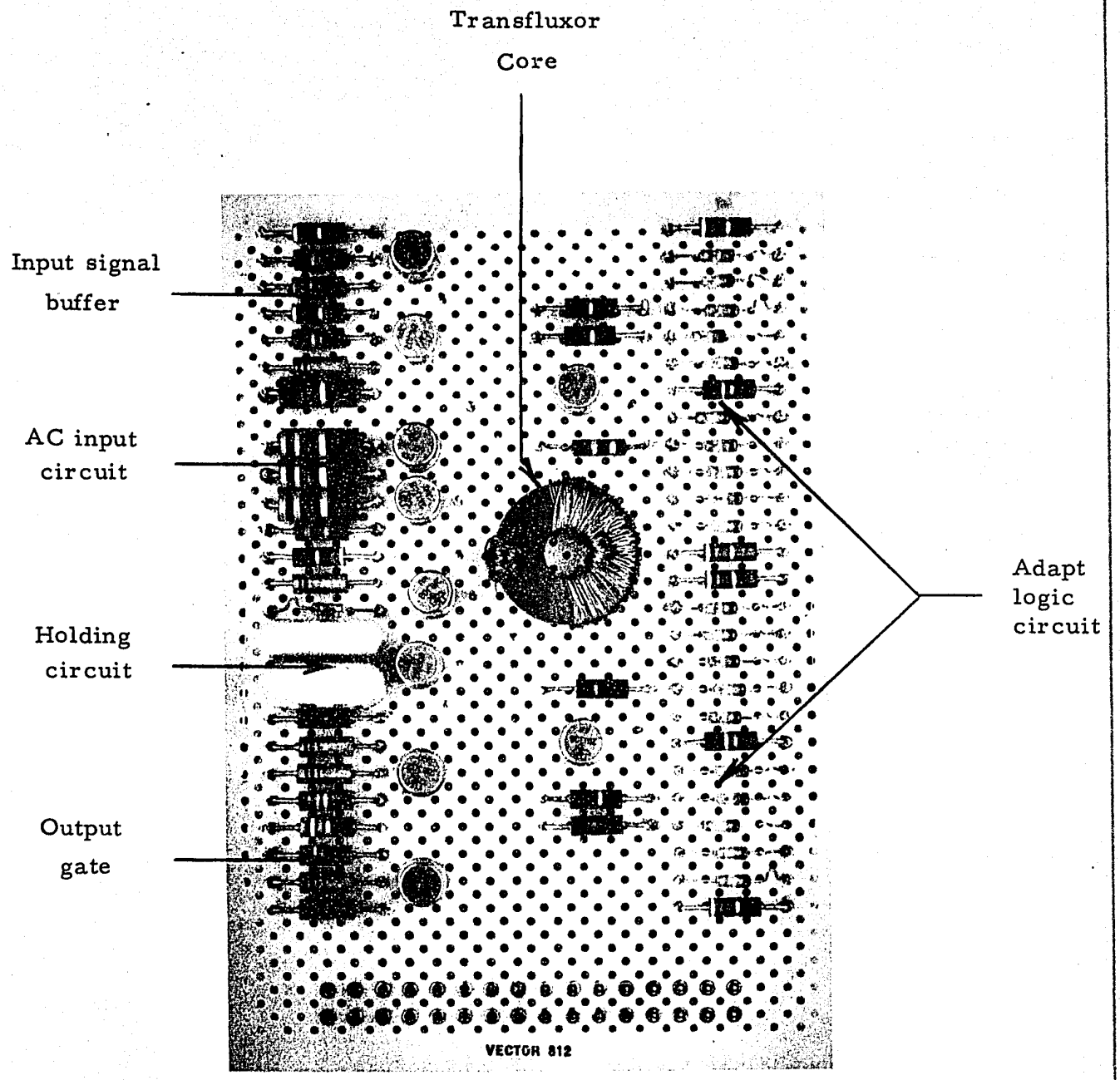

Figure 33

Adaptive Weight Unit.

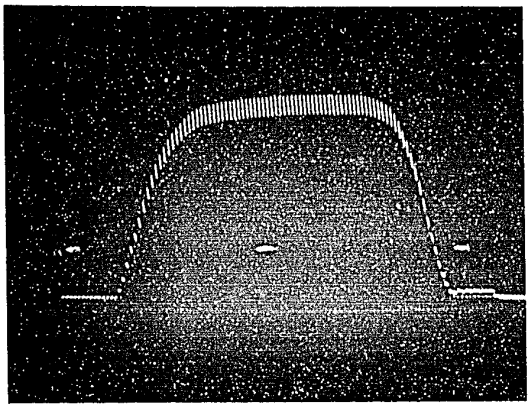

Weight Unit Number 1

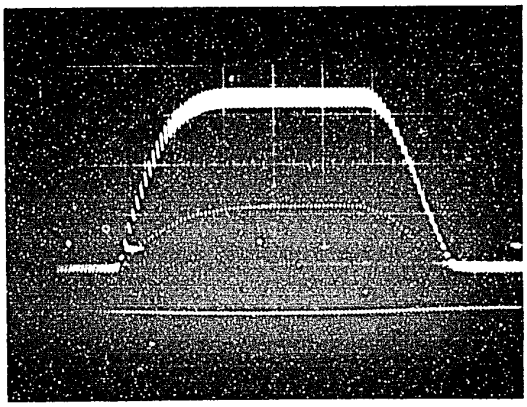

Weight Unit Number 2

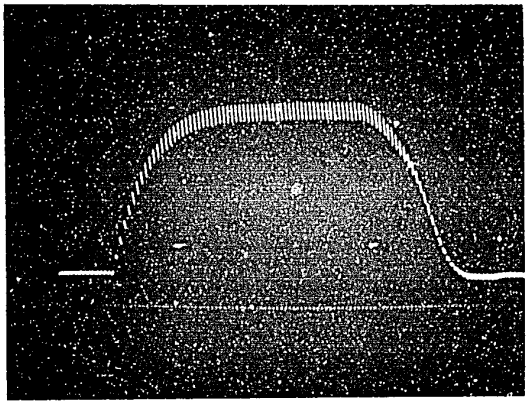

Weight Unit Number 3

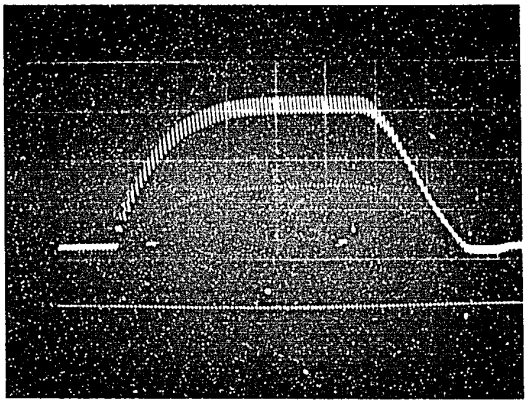

Weight Unit Number 4

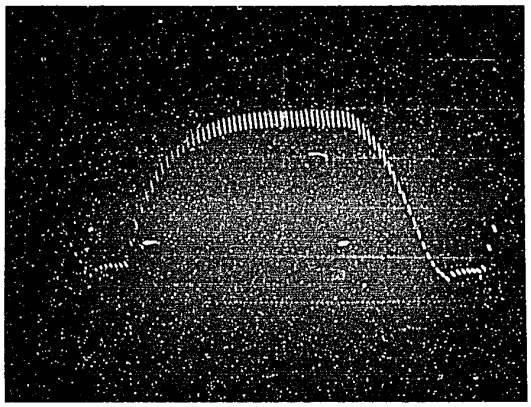

Weight Unit Number 5

Figure 34

Operating Characteristics of Weight Units

vertical scale: 5 volts/div.

Weight Unit Number	Lower Voltage Limit (Volts)	Upper Voltage Limit (Volts)	Approx. No. of Steps on Positive Slope	Approx. No. of Steps on Negative Slope	Increment Voltage Amplitude E_I (Volts)	Decrement Voltage Amplitude E_D (Volts)
1	2	22	25	21	1.8	2.2
2	5	23	22	21	1.6	2.2
3	3	21	25	24	1.5	2.6
4	6	21	28	25	1.2	2.0
5	4	20	25	21	1.5	3.4

Figure 35

Summary of Important Weight Characteristics.

Input x_1	Input x_2	Functions 0	1	2	3	4	5	6	7	8	9	10	11	12	13	14	15
0	0	0	0	0	0	0	0	0	0	1	1	1	1	1	1	1	1
0	1	0	0	0	0	1	1	1	1	0	0	0	0	1	1	1	1
1	1	0	0	1	1	0	0	1	1	0	0	1	1	0	0	1	1
1	0	0	1	0	1	0	1	0	1	0	1	0	1	0	1	0	1
No. of Adaptations		0	1	4	1	1	-	3	5	1	2	-	2	2	3	6	3

Figure 36

Two-Input-Case Test Results.

Inputs			Functions						
x_1	x_2	x_3	0	1	2*	3	4*	5	6
0	0	0	0	0	1	1	0	1	0
0	0	1	0	0	0	0	0	0	0
0	1	0	0	0	0	1	0	1	0
0	1	1	0	1	0	1	0	0	0
1	0	0	0	1	0	1	0	1	1
1	0	1	1	1	0	0	1	1	1
1	1	0	1	1	0	1	1	1	1
1	1	1	1	1	1	1	0	1	1
Realizable ?			No	No	No	Yes	No	Yes	Yes

* non-realizable functions

Figure 37

Thre-Input-Case Test Results

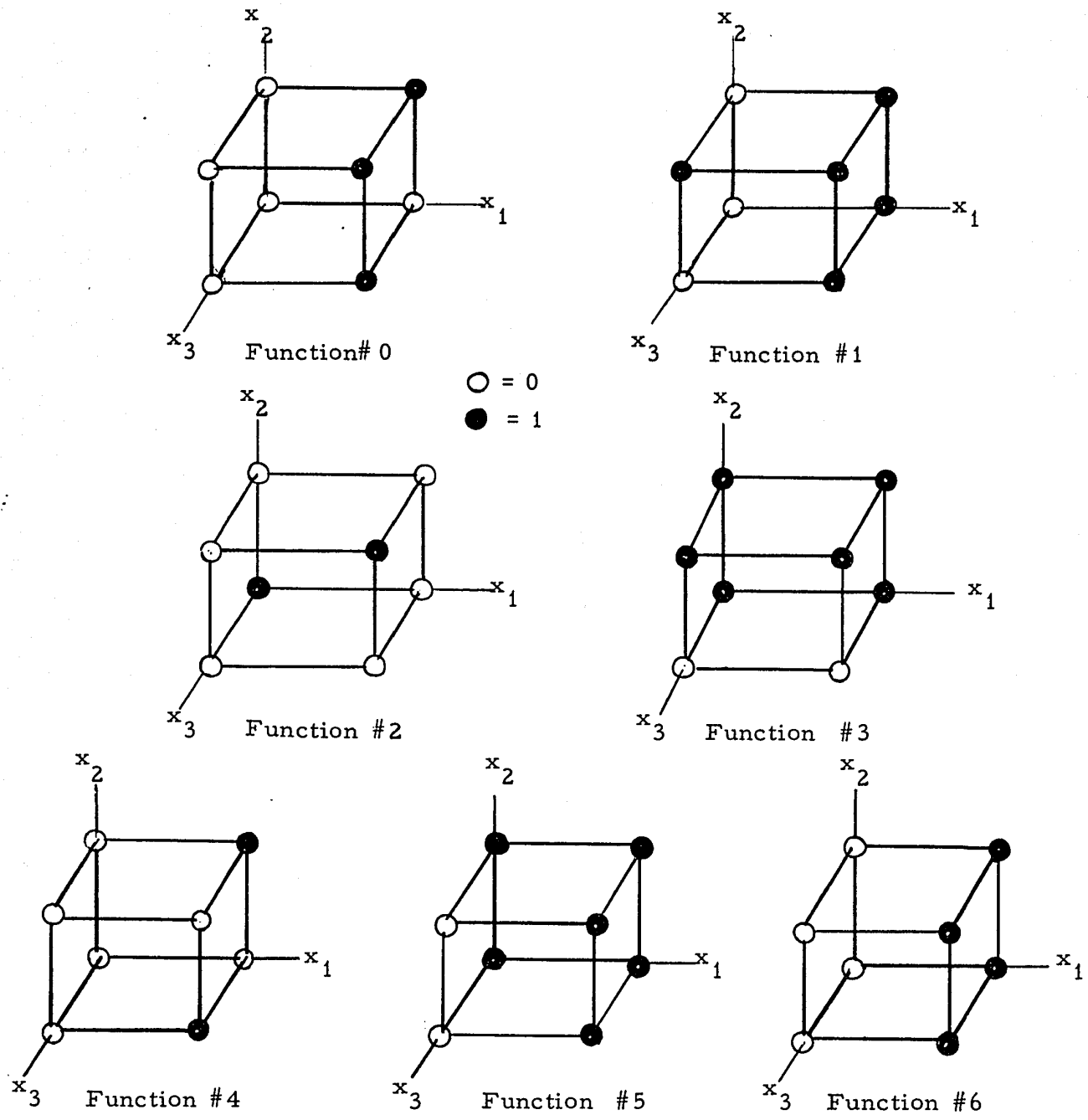

Figure 38. Three-Dimensional Projection of the Three-Input-Case Functions.

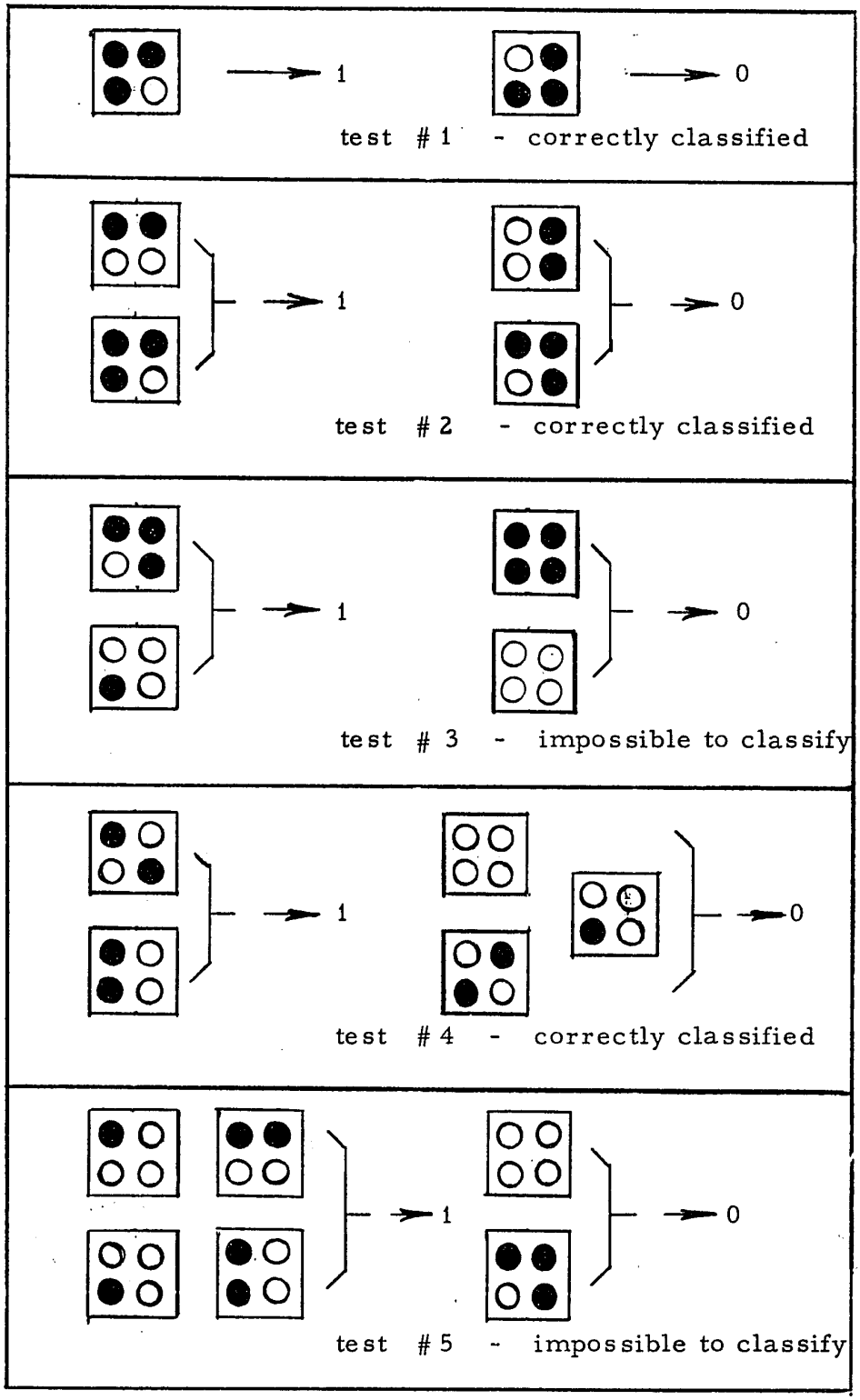

Figure 39
Four-Input-Case Test Results.

REFERENCES

1. Deschenes, P.A., "Development of an Adaptive Threshold Element", M.Sc. Thesis, University of Ottawa; 1963.

2. Winder, R.O., "Threshold Logic," Ph.D. Thesis, Princeton University; 1962.

3. Minnick, R., "Linear - Input Logic," IRE Trans. on Electronic Computers, PGEC-10 Number 1, March 1961; pp 6-16.

4. Glinski, G., and Yue, C.K., "An Introduction to Threshold Logic Functions" Technical Report No. 63-3, University of Ottawa; June, 1963.

5. Rosenblatt, F., Principles of Neurodynamics: Perceptron and the Theory of Brain Mechanisms, Spartan Books, Wash., D.C.; 1961.

6. Rosenblatt, F., "Perceptron Simulation Experiments", Proc. IRE, vol. 48, March 1960; pp 301.

7. Joseph, R., "Contributions to Perceptron Theory", Report No. VG-1196-G-7, Cornell Aeronautical Laboratory; 1960.

8. Widrow, B., and Angell, J., "Reliable, Trainable Networks for Computing and Control", Aerospace Engineering, vol. 21, No. 9, Sept., 1962.

9. Widrow, B., and Hoff, M.E., "Adaptive Switching Circuits," Technical Report No. 1553-1, Stanford Electronics Laboratory, June 30, 1960; pp. 2.

10. Widrow, B., "Adaptive Sampled-Data Systems - A Statistical Theory of Adaptation", 1959 IRE, WESCON Convention Record, Part 4; pp. 74-85.

11. Rosenblatt, F., "On the Convergence of Reinforcement Procedures in Simple Perceptrons," Report No. VG-1196-G-4, Cornell Aeronautical Laboratory; 1960.

12. Matson, R., "A Self-Organizing Logical System," Proc. of E.J.C.C. Dec., 1959.

13. Matson, R., "An Approach to Pattern Recognition Using Linear Threshold Devices", Technical Report No LMSO-702 680, Lockheed Missiles and Space Division, Sunnyside, Calif. ; Sept., 1960.

14. Nagy, G., "A Survey of Analog Memory Devices", IEEE Trans. on Electronic Computers, PG EC-12, No. 4, Aug., 1963; pp. 388.

15. Rajchman, J.A., and Lo, A.W., "The Transfluxor - A Magnetic Gate with Stored Variable Setting, RCA Review, vol 16, June, 1955; pp 303-311.

16. Rajchman, J.A., and Lo, A.W., "The Transfluxor", Proc. of IRE, vol. 44 No. 3, March, 1956; pp 321-329.

17. Hamaoka, F., and Sakao, M., "Pulse Counter Incorporating Transistors and Magnetic Core," Mitsubishi Denki Laboratory Report, October, 1962; pp. 422-445.

18. Quartly, C.J., Square-Loop Ferrite Circuitry, Prentice-Hall Inc., Englewood Cliffs, New Jersey, 1962.

19. Winder, R.O. "Threshold Logic", Ph.D. Thesis, Princeton University, 1962; pp. 143.

20. Myhill, J. and Kautz, W., "On the Size of Weights Required for Linear Input Switching Functions, IRE Trans on Electronic Computers, PGEC-10, No. 2, June, 1961; pp 288-290.

21. Crafts, H.S., "Components That Learn", Electronics, March 22, 1963; pp. 49-53.

22. "Electronic Realization of Functional Nerve Nets", Technical Documentary Report ASD-TDR-62-266, Melpar, Inc., 3000 Arlington Blvd., Falls Church, Virginia, March 1962 pp. 75.

23. Brain, A. E., "The Simulation of Neural Elements by Electrical Networks Based on Multi-Aperture Magnetic Cores", Proc. of IRE, vol. 49, No. 1, Jan., 1961; pp. 49-52.

24. Morgan, W. L., "Transfluxor Design Considerations", IRE Trans on Electron Devices, vol ED-8, No. 2, March, 1961.

25. Low, P. R., "The Influence of Component Imperfections on Trainable Systems Performance" Technical Report No. 4654-1, Stanford Electronics Laboratory, Oct., 1963.

26. Mays, C. H., "Adaptive Threshold Logic" Report SEL-63-027 (TR No 1557-1) Stanford Electronics Labs., Stanford, Calif. Feb. 1963.

VITA

Name:	Robert James Tarry
Date of birth:	18 February 1938
Place of birth:	Regina, Saskatchewan

Education:

High School	Winnipeg Technical - Vocational High School
Pre-engineering	United College Winnipeg, Manitoba
Training in Electronics	Royal Canadian Air Force Radar and Telecommunications School, Clinton, Ontario.
B.Sc (E.E.)	University of Manitoba.